École polytechnique de Louvain

Analyzing retail pricing options in distribution systems

Author: **Jacques-Marius Roland**
Supervisor: **Anthony Papavasiliou**
Readers: **Pierre-Antoine Absil, Raphael Jungers**
Academic year 2018–2019
Master [120] in Mathematical Engineering

Abstract

This master thesis studies the ecological expansion of electricity distribution systems.

At first, we will examine a distribution system situated in the Californian Bay area. Its network structure and topological characteristics are extracted in order to generate a typical distribution system feeder using duplication of certain network structures.

The second part of the thesis is devoted to a new framework for designing low voltage parts of a distribution system when customers are allowed to install photo voltaic (PV) systems. A convex multi-stage perfect foresight optimization problem minimizing the system annuity is then proposed and solved based on the framework's assumptions. This optimization problem computes how much complementary technologies have to be installed next to the chosen PV systems. The results tell us that the battery energy storage system (BESS) construction is prioritized as it reduces the development of the needed maximal power capacity of the low voltage lines.

Finally, the customer behavior is studied as a response to flat rate, time of use and real time retail pricing using linear and convex multi-stage stochastic optimization problems. Flat rate and time of use pricing induce inappropriate customer response while real time pricing results in ecologically efficient network and enhanced financial behavior.

Acknowledgements

First of all, I would like to thank my supervisor, Anthony Papavasiliou. You have learnt me a lot regarding research. I am very thankful for the time you devoted to me and have really enjoyed working with you. You always made time available for me even when it was difficult for you. I hope we will continue collaborating in the future.

Next, I would like to thank Ilyes Mezghani for helping me with my implementation problems. I hope we will see each other more often in the future. My thanks also go to Taku Kaneda and Daniel Felipe Avila Girardot, I have enjoyed working with both of you.

I would like to express my gratitude to Pierre-Antoine Absil and Raphael Jungers for being part of my master thesis jury.

Finally, my thanks go to my family who have supported me throughout my entire life. I thank my mother for having introduced me to operational research and motivated me towards academic research, I am very proud of what you achieve. I thank my father for raising me and helping me on every possible occasion. I am very happy that you raised me and hope I will be able to return the favor in the future.

Contents

List of Figures

List of Tables

Acronyms

BESS Battery Energy Storage System

DSO Distribution System Operator

EHV Extra High Voltage

EV Electric Vehicles

HV High Voltage

LCT Low Carbon Technologies

LV Low Voltage

MSP Multi-stage Stochastic Problem

MV Medium Voltage

PF Power Flow

PV Photo Voltaic

RES Renewable Energy Sources

RT Real Time

TSO Transmission System Operator

Introduction

Motivation

The recent discoveries related to climate change have shown that the way we deal with energy has to evolve. These discoveries lead to social as well as political reactions inducing radical changes in mentalities around the earth. In the field of energy three main bottlenecks can be identified in order to make this transition towards a reduced ecological footprint feasible.

The first step towards this evolution is related to the **production of energy** which has traditionally been done using fossil fuels. These resources are limited and their reserves are decreasing from day to day. This part is being extensively studied from multiple scientific point of views and alternatives such as Renewable Energy Sources (RES) are constantly improved through research. Countries such as Germany have already been able to highly increase their renewable energy production, now representing 30 % of their total power mix [5]. Individual customers are now also encouraged to participate to the efficient production of energy by installing RES to reduce their own ecological footprint and electrical bill.

The second step corresponds to how we **consume energy**. A change in mentality can now be observed from the consumer point of view. Indeed, the awareness of the consumer for climate change has evolved and many individuals are doing their best to reduce their ecological footprint. In [6] we see that in most countries at least 70 % of the population is aware of climate change and the threat it represents for humanity. This also influences the vision of many companies which are trying to reduce their own ecological footprint for ethical reasons and also in order to induce a positive customer image. Initiatives to influence car brands to design Electric Vehicles (EV) as well as consumer discounts on EV's are also currently growing in popularity in many countries.

The final, generally forgotten, highly relevant step towards an ecological transition is the **efficient dispatch of energy**. It is not only sufficient to adequately produce and consume energy, it is also important to bring this energy to the individual consumer in an efficient way. The electricity supply chain (connecting generators with consumers) stands at the center of this transition. New network technologies such as micro grids, distributed generation, battery energy storage systems and consumer photo voltaic panels are changing the way these systems have to be planned and designed. The electricity supply chain (also called power system) is depicted in Figure 1. It has traditionally been divided in three parts:

1. Production: Here the electricity is generated, usually through the use of power plants. These plants can generate electricity using a multitude of methods going from the combustion of fossil fuels to the use of potential energy extracted from water originating from rivers and dams. This raw electricity is usually obtained at Extra High Voltage (EHV).

2. Transmission: Once the electricity has been generated it needs to be brought to the customers who can be situated at a large distance from the source. In order for this to be done the generated electricity is transformed to High Voltage (HV) reducing transportation losses due to the Joule effect.

3. Distribution: After it has been transported over high distances, the electricity arrives at the distribution substation which transforms it into Medium/Low Voltage (MV/LV) so as to distribute it in the area close to the substation. Generally, distinction is made between urban, sub-urban and rural area. The customers who can be industrial, commercial or residential connect to the different parts of the distribution system depending on the quantity of power withdrawn from the network.

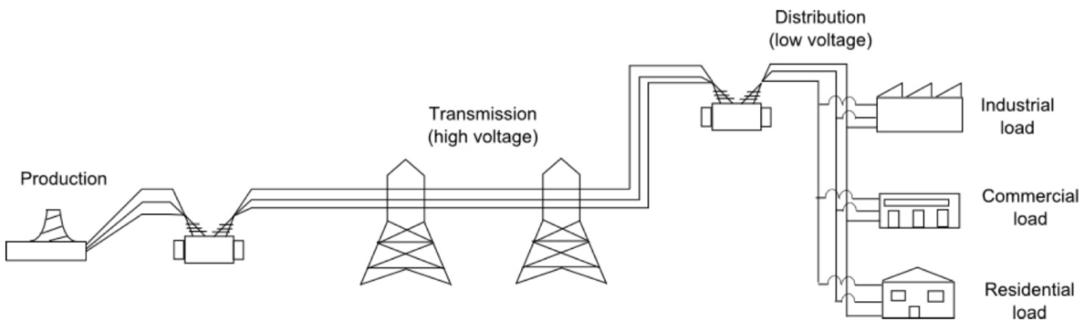

Figure 1: The electricity supply chain (taken from [1]).

Objectives

Two different topics are considered in this thesis.

The first one addresses the need for realistic distribution system instances to test optimal dispatch models and algorithms. Indeed, as research of the electricity supply chain has been moving towards the study of distribution systems it has been important to be able to test developed models and methods on some realistic test instances which are very scarce at the moment.

The second one investigates power systems from an economical point of view using mathematical optimization. By enhancing the electrical supply chain with new technologies, the individual consumer will be in a position to make appropriate decisions to control his energy exchange with the network. He will indeed be able to reduce his payment by injecting energy into the network at the right time. More specifically, the attention will be focused on the design and retail pricing of distribution systems as a response to changes in customer behavior. The following questions will be addressed and answered:

1. How should a low voltage subnetwork optimally be designed in order to maximize the power system welfare?
2. How will distribution system customers equipped with a PV system and a BESS react to different retail pricing options?
3. What are the consequences from a network point of view of high RES penetration at consumer level?

State of the art

The approach considered in this thesis focuses on how low voltage parts of distribution systems need to be designed for the integration of RES. One should note that the framework that will be presented in this thesis is new and does not rely on many pre-existing studies.

So far, research about the design of distribution systems has merely been studied from a feeder, thus larger, framework. In [7] the impact of batteries on distribution substations is studied using the maximization of the net present value of the system. A multi objective nonlinear problem formulation is proposed and solved using nondominated sorting genetic algorithms. A similar approach is also taken in [8] but here, the reinforcement of transformers, lines, capacitors and installation of distributed generation is considered. This model considers a detailed version of the network and solves the non linear problem using modified discrete particle swarm optimization. Both articles suppose that the demand is a deterministic component. Low voltage network design has however been investigated from a geographical point of view in the past. In [9] a model is proposed based on evolution strategies in order to plan the geographical expansion of low voltage parts of distribution systems. Recently an economical study of a micro grid situated in Garowe, Somalia as been made in [10]. This article studies the performance of two micro grid energy management systems and what the optimally installed PV system capacity and BESS capacity should be in order to minimize the system annuity.

The influence of integrating Low Carbon Technologies (LCT) on distribution system feeders has been studied from a network stability point of view in [11]. Consequences on voltage issues and line congestion are studied by making simulations using typical demand and PV system power output data. The different pricing options for distribution systems have also been investigated using economical principles in [12] without taking into account the impact of LCT. The reactions of households to dynamic pricing as well as other consequences of using dynamic pricing are studied using available statistical data. In [13] a discussion is made on progress, opportunities, and issues related with dynamic pricing.

Other mathematical approaches have also been taken. In [14] a stochastic bi-level model is set up in order for the DSO and Retailer to maximize their net present value by optimally choosing prices for the entire network. The customers defined by a demand response model are here seen as the followers whereas the DSO and Retailer represent the leader. The model is solved by integrating the KKT conditions of the follower model into the leader model and casting the problem as a mixed integer linear problem.

Overview of the thesis

In Chapter 1 the necessary theory about distribution systems will be presented as well as the mathematical theory needed to understand the subsequent chapters. Then, in Chapter 2 a typical distribution system will be studied from a structural and topological point of view in order to easily generate typical distribution system instances and understand their characteristics. This will allow us to set up a new framework for designing and studying low voltage parts of distribution systems in Chapter 3. And finally, with the results of Chapter 4, we will establish the optimal behavior to be adopted by distribution system customers as a response to different retail tariff options.

Chapter 1

Preliminary notions about distribution systems and mathematical concepts

1.1 Distribution systems

Distribution systems typically have a radial structure (e.g. a tree structure). The energy generally arrives at the root of the system using transmission lines and is then redistributed to the customers through the branches of the distribution network.

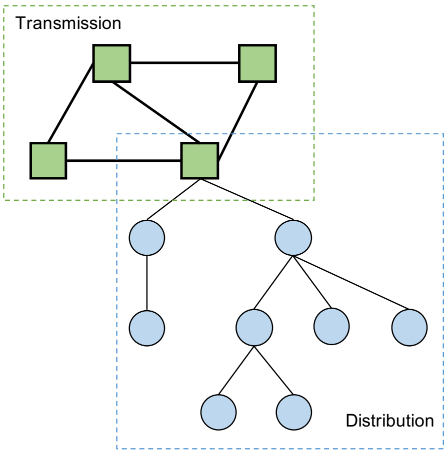

Figure 1.1: Radial distribution system illustration.

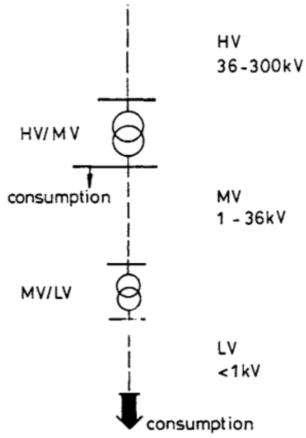

Figure 1.2: Block schematic of a distribution system (taken from [2])

These systems are usually divided into three parts:

1. Distribution substation: The high voltage electricity first arrives at the distribution substation through transmission lines where it is downgraded to medium voltage. The distribution substation corresponds to the HV/MV transformer in Figure 1.2.

2. Medium voltage level (1 - 36 kV): Here, some large customers can be connected (for example the railway, large industrial partners, etc). The electricity is then transported

over a defined region in order for it to be in close range of the individual customers. This part is often called primary distribution.

3. Low voltage level (< 1 kV): Once the medium voltage level is close enough to the individual customer the electricity is stepped down to low voltage using step down transformers. This low voltage level then connects the individual customers which are situated close to the step down transformer. The length of new LV lines is usually limited to around 500 m or even less [2]. This part is often called secondary distribution or low voltage supply.

A distribution feeder is then defined as a subnetwork rooted at the distribution transformer. It always contains one medium voltage level connected to multiple step down transformers which connect to individual customers. As low voltage induces more losses compared to medium voltage it is preferred to maximize the span of the primary distribution in order to reduce the use of low voltage cables [15]. The medium voltage part will therefore usually contain more buses and cables compared to low voltage. Normally, multiple feeders take their root at the distribution substation. These feeders are usually designed in order to satisfy the demand of a specific area. One also has to note that the transformers correspond to the gates between voltage levels.

1.1.1 Organization of electricity distribution in Belgium

The price written on our electricity bill is a mystery for an important fraction of the Belgian population. That is most likely due to the fact that the way distribution systems are operated is more complicated than it looks. The bill you pay originates from two separate operations done in order to bring the electricity to your residence. First, there is the price of electricity you buy from a retailer of your choice (e.g. Engie, Mega, etc..). The retailer is responsible for the generation, storage and retailing of the electricity and thus has to make sure that electricity is always available. This first component will thus be competitively adapted to the market.

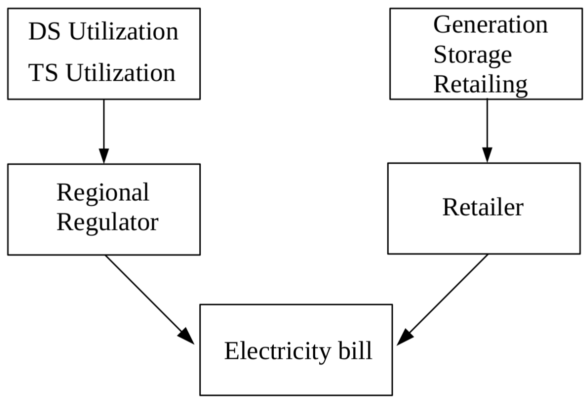

Figure 1.3: Organization of distribution systems and influence on the electricity price.

The second component, which originates from the electricity supply chain, is due to the utilization of the transmission and distribution systems. These systems are unique and operated by the Transmission System Operator (TSO) and the Distribution System Operator (DSO) which own the assets and thus posses a natural monopoly. In order for the DSO and TSO to not be able to take advantage of their monopoly it has been decided that this price component is decided by state held regional regulators. These regional regulators were created in the early 2000s because operators are subject to regulatory oversight by a European directive implemented in Belgian law due to their natural monopoly [16]. However, as mentioned previously, these operators often only posses the infrastructure and do not deal with the day to day operation of the systems which they delegate to legally separate service companies.

Two actors can thus be identified in our case. The retailer, whose objective is to maximize his profit while avoiding black outs at all costs and the DSO which is responsible for the proper operation of the distribution system.

1.1.2 A contradictory aspect of the distribution systems

With the growing numbers of PV systems and batteries two major issues will arise in the organization of distribution systems. These technologies indeed allow the individual consumer to control his interaction with the grid. Giving him the possibility to inject excess power in the grid in return of a reduced bill at the end of the month. At first sight this looks like a way of reducing power shedding as this excess power can be redistributed to other, more consuming, consumers.

However, the way we price electricity will influence this customers behavior. He will indeed more likely inject power during a period with higher return price thus increasing the chance of having multiple consumers injecting electricity at the same time. Because DSO's are unable to posses storage facilities by law, this might lead to oversupply which will eventually have to be thrown away. The other drawback of this democratization of PV systems and BESS is the fact that feeders have been designed given a maximal power the lines have to withstand. The customers will most likely try to minimize their bill at the end of the month without taking this into account. The influence of these new technologies will induce similar customer behavior thus increasing the risk of line saturation. The retail pricing methods represent here the key to controlling and estimating the customer behavior.

1.2 Mathematical concepts

Some relevant mathematical concepts for the next chapters will now be presented.

1.2.1 Stochastic optimization

Stochastic optimization is the branch of optimization that is concerned with problems influenced by uncertain parameters. Two typical ways of tackling these problems are presented and will be used in subsequent chapters.

Multi-stage stochastic optimization

We suppose that the system can be described using a Markov decision model. This means that given a set of time steps $T = \{0, \ldots, H\}$ we suppose that the realization of uncertainty of the system, denoted by ξ, can fully be characterized by a set of nodes $w_t \in \Omega_t$. These nodes correspond to individual realization of ξ where Ω_t represents the set of all nodes in time step t. From the definition of the Markov decision process it comes that the probability of going to a specific node at the next time step does not dependent of the previous realizations of uncertainty but only of the current realization of uncertainty

$$\mathbb{P}(w_{t+1}|w_t, \ldots, w_0) = \mathbb{P}(w_{t+1}|w_t) \quad \forall t \in T \setminus \{H\}, \forall w_t \in \Omega_t, \forall w_{t+1} \in \Omega_{t+1}.$$

This can be visualized using two models called the lattice representation and the scenario

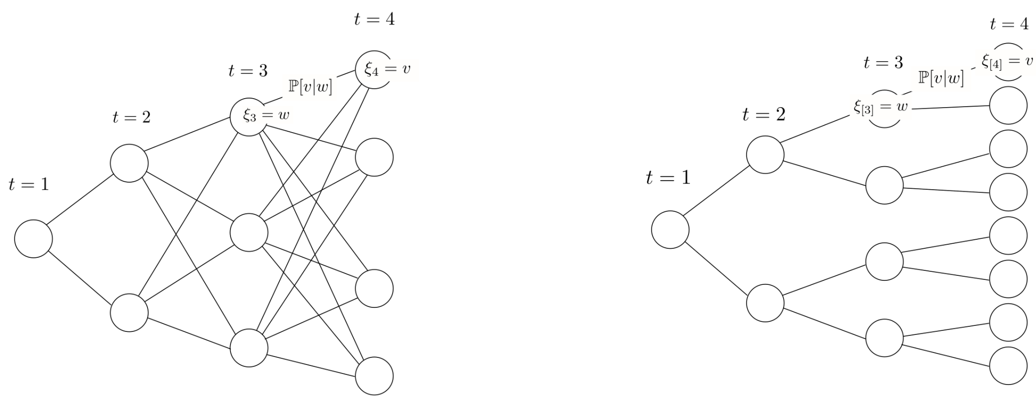

(a) Lattice

(b) Scenario tree

Figure 1.4: Uncertainty representations (taken from [3]).

tree representation as shown in Figure 1.4. Where the nodes of the scenario tree correspond to histories of random realizations such that

$$\begin{aligned} \xi_{[t]} &= (\xi_0, \ldots, \xi_t), \\ w_{[t]} &= (w_0, \ldots, w_t). \end{aligned}$$

The set $\Omega_{[t]}$ is then defined as the set of all possible scenarios in time step t. We define $a(w_{[t]})$ as the ancestor of $w_{[t]}$, thus meaning that if

$$w_{[t]} = (w_0, \dots, w_t),$$

then

$$a(w_{[t]}) = (w_0, \dots, w_{t-1}),$$

where the the ancestor of a certain scenario can also be the ancestor of another scenario in the same time stage. It should be noted that Ω_t and $\Omega_{[t]}$ are not the same and respectively represent the nodes assigned to individual uncertainty realizations during one time step and the nodes assigned to all possible histories of random realizations until time step t.

The scenario tree representation thus represents a way to consider all sequences of uncertainty realizations from time step zero to time step t using nodes. These nodes are interconnected by edges representing the transition probabilities between these sequences. The lattice model represents a way to consider all individual realizations of uncertainty for each time step modeled by nodes. These nodes are then also interconnected by edges representing the transition probabilities between these uncertainty realizations. The lattice representation is a compact version for displaying the realizations of uncertainty whereas the scenario tree representation may contain an exponential number of nodes. It should be noted that one can easily switch between both representations using basic probability theory.

Multi-stage stochastic problem

A set of stage and action variables $x = [x_0, \dots, x_H]$ are defined. They respectively correspond to the variables describing the state of the system (the state of a system can for example be the energy level of a battery which will change throughout the time-stages) and to the decisions influencing the future state of the system (for example how much we charge a battery which will change the energy level of the battery in the following period). We define a policy as a function returning an decision based on the considered scenario of the scenario tree. The cost function $C_t^{w_{[}t]}$ defined such that

$$C_t^{w_{[t]}}(x_t^{w_{[t]}}) : \mathbb{R} \to \mathbb{R} \quad \forall t \in T, \forall w_{[t]} \in \Omega_{[t]},$$

represents the cost at time step t if the system is in node $w_{[t]}$ of the scenario tree and decision $x_t^{w_{[}t]}$ is made.

Having defined the necessary concepts used for modeling the uncertainty and decisions we define a Multi-stage Stochastic Problem (MSP). This problem returns the optimal policy used to minimize the expected cost of the system over the considered horizon (from time step 0 to time step H). If we define W_t as the current stage coefficient matrix, T_t as the previous time stage decision coefficient matrix and $h_t^{w_{[t]}}$ as the current stage realization of uncertainty in scenario $w_{[t]}$ we obtain Model 1. Objective 1.1a corresponds to the minimization of the expected cost over the considered horizon while constraint 1.1b links the decision variables at subsequent time stages.

Model 1: Multi-stage stochastic optimization problem.

$$\begin{aligned}
\underset{x}{\text{minimize}} \quad & \sum_{t\in T} \sum_{w_{[t]}\in\Omega_{[t]}} \mathbb{P}(w_{[t]}) C_t^{w_{[t]}}\big(x_t^{w_{[t]}}\big) && && (1.1a)\\
\text{subject to} \quad & W_t x_t^{w_{[t]}} = h_t^{w_{[t]}} - T_t x_{t-1}^{a(w_{[t]})}, && t \in T, w_{[t]} \in \Omega_{[t]}, && (1.1b)\\
& x_t^{w_{[t]}} \geq 0, && t \in T, w_{[t]} \in \Omega_{[t]}.
\end{aligned}$$

It should be noted that linear constraints are considerd while the objective can be non-linear depending on the definition of function $C_t^{w_{[t]}}(x_t^{w_{[t]}})$.

Multi-stage perfect foresight problem

Another approach can also be taken to study these types of problems. This approach is called the perfect foresight and consists in sampling a fixed amount of scenarios in the scenario tree. The decisions have then to be made on the individual scenarios meaning that the uncertain parameters are now considered as deterministic for each scenario. The mean scenario cost is then minimized over the considered horizon. This model is useful for comparing the stochastic model with the fact of having perfect information about the future uncertainty realizations. It can however difficultly be used for making real time decisions. Let S be the set of of sampled scenarios through the scenario tree. We keep the notation of Model 1, giving us Model 2.

Model 2: Multi-stage perfect foresight optimization problem.

$$\begin{aligned}
\underset{x}{\text{minimize}} \quad & \sum_{t\in T} \sum_{s\in S} \frac{1}{|S|} C_t^s\big(x_t^s\big) \\
\text{subject to} \quad & W_t x_t^s = h_t^s - T_t x_{t-1}^s, && t \in T, s \in S, && (1.2a)\\
& x_t^s \geq 0, && t \in T, s \in S.
\end{aligned}$$

It should be noted that constraint 1.2a will only link the subsequent decisions of the same sampled scenario while this will link all ancestor scenarios to the considered scenario in constraint 1.1b.

1.2.2 Competitive markets and economic dispatch

The competitive market model is presented from a mathematical point of view and classical results will be deduced in order to derive retail prices in Chapter 4.

Let A define a set of n agents exchanging resources. These resources are often referred to as commodities representing scarce resources that are traded without differentiation at a single market price, denoted by λ. Let the considered market be a competitive market as defined in [1].

Definition 1.2.1. Competitive market: A market is competitive if the following conditions hold:

- Agents are price-taking. Mathematically, this means that when agents maximize profit they consider price as a fixed parameter in their optimization, rather than a decision variable that can be influenced by their actions.
- The variable costs of producers are convex, equivalently their marginal costs are increasing. Analogously, the total benefit of consumers is concave, equivalently the marginal benefit of consumers is decreasing.
- Agents are fully informed about the market prices.

We suppose that each agent makes a set of decisions x_a in $\mathbb{R}^{t_a}$ which will influence the quantity of exchanged resources, denoted by q_a which is positive if they are bought and negative if sold. Let $f_a(x_a)$ represent the individual customer benefit function. We also define

$$g_a(x_a) \leq 0$$

a set of constraints specific to agent a and

$$h_a(x_a) = q_a$$

a set of resource allocation constraints depending on the agent. Functions $f_a(x_a), g_a(x_a)$ and $h_a(x_a)$ are convex. A final constraint is then added in order to model the exchange of goods between agents, this constraint is called the market clearing condition and is defined such that

$$\sum_{a \in A} q_a \leq 0,$$

which means that more resources are sold compared to procured resources. The profit maximization of agent a is then defined as in Model 3. He tries to find a solution maximizing his personal welfare while satisfying his own constraints. The economic dispatch problem, which can be found in Model 4, is defined such that total welfare of the system is maximized while satisfying all the agent's constraints and the market clearing constraint.

Model 3: Profit maximization of agent a.

$$\begin{aligned} \underset{x_a, q_a}{\text{minimize}} \quad & f_a(x_a) - \lambda q_a \\ \text{subject to} \quad & g_a(x_a) \leq 0, \\ & h_a(x_a) = 0 \end{aligned}$$

Model 4: Economic dispatch problem.

$$\begin{aligned} \underset{x_a, q_a}{\text{minimize}} \quad & \sum_{a \in A} f_a(x_a) \\ \text{subject to} \quad & g_a(x_a) \leq 0 \quad \forall a \in A, \\ & \sum_{a \in A} h_a(x_a) = 0 \end{aligned}$$

The competitive equilibrium can then be defined similarly as in [1].

Definition 1.2.2. Competitive equilibrium: A competitive equilibrium over multiple products is defined as a set of prices λ, agent decisions x_a and commodity procurements q_a such that:

- (q_a, x_a) maximize the profit of agent a , i.e. they solve Model 3.
- market clearing holds:

$$0 \leq \lambda \perp \sum_{a \in A} q_a \leq 0.$$

The following proposition can then be proven and will be very important for later chapters.

Proposition 1.2.1. A competitive market equilibrium satisfies the KKT conditions of Model 4. Therefore, a competitive market equilibrium results in an optimal solution of 4, i.e. a globally optimal allocation of resources. The converse also holds, namely a primal-dual solution to the KKT conditions of 4 is a competitive equilibrium.

Proof. See [1]. □

This proposition thus tells us that the optimal solution of the economic dispatch problem corresponds to the individual welfare maximization of all agents as well as the market clearing constraint. It also tells us that λ will be given by the dual multipliers of the market clearing constraint.

Chapter 2

Generation of realistic distribution system instances

2.1 The need for realistic instances

As research regarding the electricity supply chain has been moving towards the study of distribution systems it became important to be able to test developed models and methods on some realistic test instances. However, as theses systems are usually a few decades old it logically comes that the amount of systems of which the size and topology ar available is really small. This number nevertheless increases due to the augmenting demand. Also, the available information often lacks some key statistics which help us to understand how these systems work. This is why, as a first step in order for us to understand them, it becomes interesting to dive deeper into their structure and to derive some features which will be used when generating new distribution systems instances. This chapter will thus serve as a guide to generate distribution system instances of given size using available distribution system data. We will therefore focus on a specific distribution system situated in the Californian Bay area of the United States. The generation of new instances will then be done using duplication of specific parts of this network.

2.2 Bay area synthetic network

The San Francisco bay area is a region situated in the north of California state in the United States. It is said to be composed of nine counties and spans over an area of 18966 km^2. Data of the distribution system in this area has been made available at [17] and has been made using the U.S. Reference Network Model (RNM-US)[18] which synthetically creates distribution systems using GIS files. This network has been generated over 7 counties and is provided in Open-DSS format (software used for the simulation of distribution system behavior).

Type	High Voltage		Medium Voltage		Low Voltage	
Voltage in network	230 kV	69 kV	12.47 kV	7.2 kV	0.48 kV	0.12 kV

Table 2.1: Identified voltage levels of the Bay area distribution network.

	0.12 kV	0.48 kV	7.2 kV	12.47 kV	69 kV	230 kV
0.12 kV	No	No	Yes	No	No	No
0.48 kV	No	No	No	Yes	No	No
7.2 kV	Yes	No	No	No	No	No
12.47 kV	No	Yes	No	Yes	Yes	No
69 kV	No	No	No	Yes	No	Yes
230 kV	No	No	No	No	Yes	No

Table 2.2: Connection of the different voltage levels via transformers.

The bay area network is composed of six different voltage levels as shown in Table 2.1. Table 2.2 shows us the connection between voltage levels and has been extracted using the transformer information. We thus see that the network follows a typical structure as illustrated in Figure 2.1. This can be deduced knowing that 0.12 kV sub networks are only connected to 7.2 kV sub networks and that 0.48 kV sub networks are only connected to 12.47 kV sub networks. As no transformers exist between the 7.2 kV sub networks and the higher voltage levels we deduced that the 7.2 kV sub networks are connected to the 69 kV sub networks. However, this lack of information results in the fact that we are not able to find the root of the 7.2 kV sub networks. This would indeed have been provided by the transformer of the distribution substation.

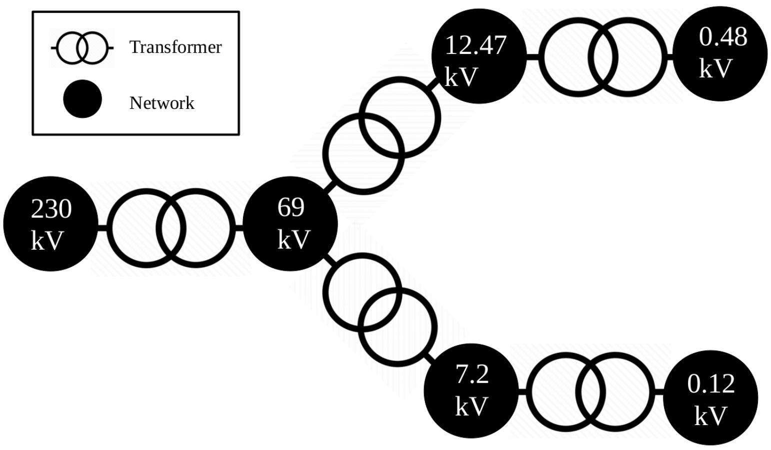

Figure 2.1: Schematic of the bay area network structure.

Figure 2.1 explains the purpose of each voltage level. First of all, the 230 kV network corresponds to the connection with transmission lines. The electricity is then stepped down to 69 kV in order for it to be transported over the Bay area. Indeed, as we are dealing with a very large region multiple distribution substations will be needed in order for the electricity to be redistributed through feeders. Once the electricity arrives at the distribution substation it is then stepped down to 7.2 kV or 12.49 kV depending on it's future use. Let us consider both possibilities:

- 12.49 kV: The electricity is then transported through one of the feeders of the primary distribution which connects to the distribution substation. Then, when it is close enough to the customer it is then stepped down to 0.48 kV which does not correspond to the voltage level of American households. An initial guess would be to think that the customer load profile will have an industrial shape.

- 7.2 kV: Again the electricity is transported through one of the feeders of the primary distribution which connect to the distribution substation. Then, when it is close enough to the customer it is then stepped down to 0.12 kV which corresponds to the voltage level of American households. The customer load profiles will thus likely look like typical household profiles.

A first observation can be made here, two separate types of consumers can be identified and are not supplied by the same feeders. This difference is of key importance when generating new instances and depends on the type of customers we want to consider. As the purpose of this chapter is to be able to generate typical distribution system instances we will only consider the generation of feeders containing 7.2 kV sub networks and the associated 0.12 kV sub networks. We are not interested by the 69 kV clusters as these correspond to high voltage lines and are not part of the distribution system. A similar methodology can of course be applied to 12.49 kV systems.

2.3 Structural aspects

In order to generate realistic instances by duplication of existing parts of the network we not only have to understand its schematic overall outer structure but also the inner structure and operation of its voltage levels. This means we would like to know of how many buses (i.e. nodes of the network), how many load buses (i.e. customers of the network represented by a node) and what type of loads (characterized by their maximal power withdrawal) are part of these networks. Thus helping us in choosing the right parts to duplicate.

This is done using clusters of nodes corresponding to sub networks of the same voltage level delimited by transformers. The clusters are created using the algorithm presented in appendix A.1 which gives us the results of Table 2.3. This algorithm creates clusters in a recursive way by continuously adding neighboring nodes until only edges corresponding to transformers are left.

Type	High Voltage		Medium Voltage		Low Voltage	
Voltage in network	230 kV	69 kV	12.47 kV	7.19956 kV	0.48 kV	0.120089 kV
Amount of clusters	1	39	13	54	40351	293035

Table 2.3: Amount of clusters per voltage level of the Bay area network.

We can immediately conclude that low voltage clusters are way more prominent compared to high and medium voltage clusters. This can be explained by the typical structure of feeders thus resulting in few very large medium voltage clusters and many small low voltage clusters. Indeed, as feeders are designed for specific areas the medium voltage part will have to reach as close as possible to the low voltage customers thus spanning over large regions and creating many low voltage clusters connected to individual step down transformers.

2.3.1 Low voltage

Figure 2.2 shows histograms of the number of buses, number of load buses and nominal load of the load buses for the 0.12 kV and 0.48 kV clusters obtained using the algorithm presented in Appendix A.1. The 0.12 kV clusters clearly correspond to households. Indeed, when looking at Figure 2.2e we can see that the nominal load of these customers exactly correspond to the typical household values. As expected, it can be noted that these voltage clusters usually contain a small amount of buses and load buses. This is highly important when trying to generate distribution system instances and will have to be taken into account.

Next, Figures 2.2a, 2.2d and 2.2f confirm our intuition about the 0.48 kV clusters. They are usually composed of two nodes, corresponding to the transformer gate and the connection with the customer (load bus). Indeed, when looking at Figure 2.2b we see that these clusters usually contain two nodes while Figure 2.2d shows us that they usually have one load bus. This can be explained by the fact that small industrial customers (farms for example) are often situated far from each other thus meaning that in order to reduce the amount of low voltage transportation there have to be many low voltage clusters. Finally, Figure 2.2f confirms our assumption by showing that the nominal load (also called peak load) of the customer achieves high values which cannot correspond to household demand but is more likely to correspond to small industrial consumers.

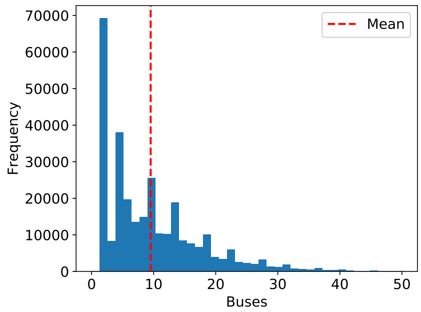

(a) 0.12 kV: Buses

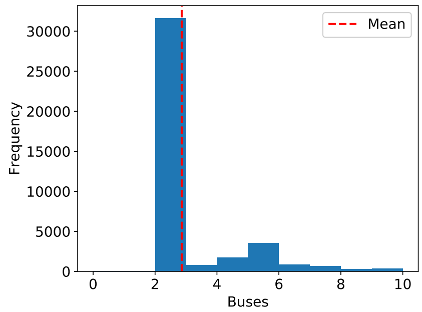

(b) 0.48 kV: Buses

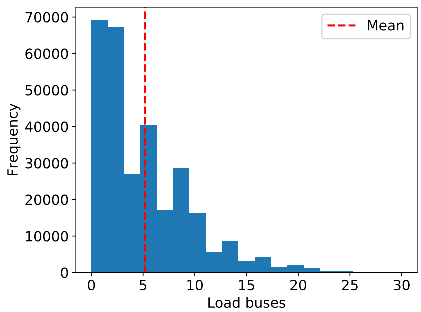

(c) 0.12 kV: Load buses

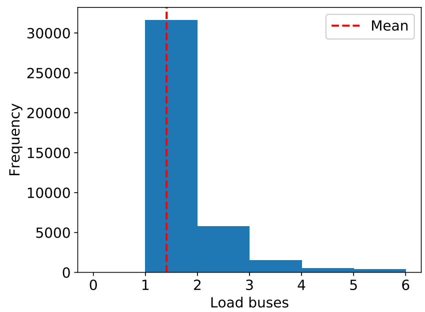

(d) 0.48 kV: Load buses

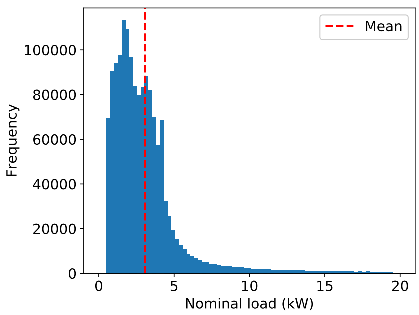

(e) 0.12 kV: Nominal load

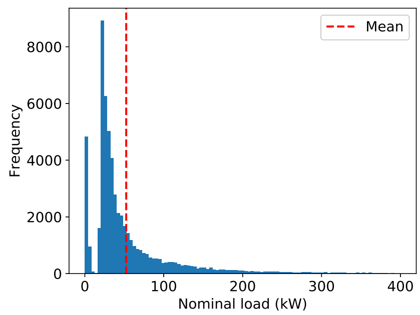

(f) 0.48 kV: Nominal Load

Figure 2.2: Histograms for the low voltage levels.

2.3.2 Medium voltage

Figure 2.3 shows histograms of the number of buses, number of load buses and nominal load of the load buses for the 7.2 kV and 12.47 kV clusters obtained using the algorithm presented in Appendix A.1. Figures 2.3a and 2.3b show us that the medium voltage clusters contain a high amount of buses. This supports the explanation of the previous section and confirms that the bay area distribution network uses indeed the typical feeder structure. The medium voltage clusters usually have zero or a small amount of load buses as shown in Figures 2.3c and 2.3d. These loads correspond to heavy industrial profiles (railways for example). This is confirmed by Figures 2.3e and 2.3f which show very high values for their nominal loads.

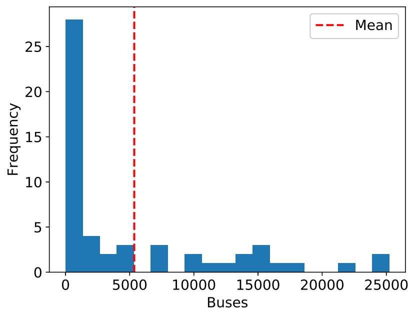

(a) 7.2 kV: Buses

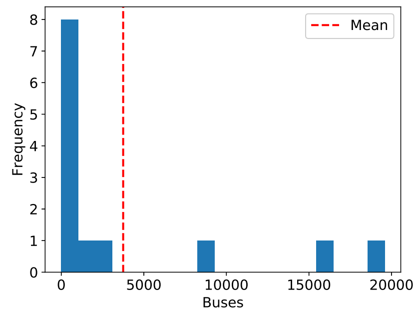

(b) 12.49 kV: Buses

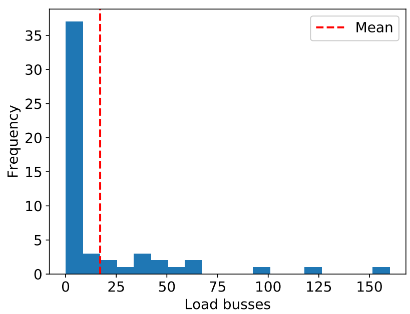

(c) 7.2 kV: Load buses

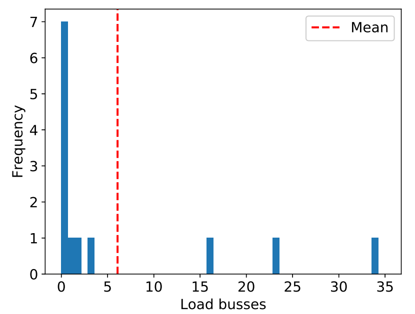

(d) 12.47 kV: Load buses

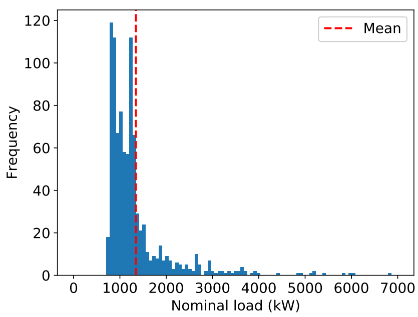

(e) 7.2 kV: Nominal Load

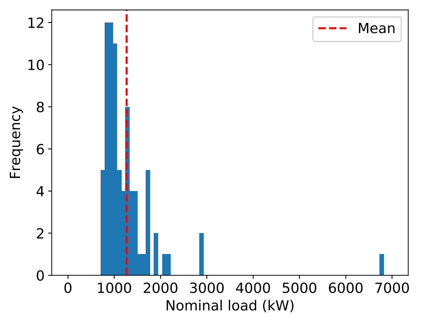

(f) 12.47 kV: Nominal Load

Figure 2.3: Histograms for the medium voltage levels.

2.4 Network generation

As we now understand the structure and topology of the bay area network there is still one question that remains unanswered: *How do we generate realistic distribution system instances?*. In other words, what makes a network a real distribution system and what are the characteristics we should be looking for. As we are trying to generate typical structures using existing network components we will have to decide which components of the clusters we will duplicate and identify the important features these components should have:

- Medium voltage should be a concatenation of typical radial feeder structures which take their root in the same bus. The interesting components here become the individual feeders of each medium voltage level and will thus be the duplicated medium voltage part.

- Low voltage should be connected via a transformer to each transformer gate of the medium voltage feeders. The template component thus represents the entire low voltage cluster. This cluster should have the typical LV network inner structure as explained in the previous section.

2.4.1 Low Voltages

Figures 2.4a and 2.4b show two typical low voltage clusters of the distribution system. We can clearly identify a radial structure. The root has been identified using the step down transformer. This, again, confirms that the primary purpose of low voltage is to connect the customer to the medium voltage over small distances.

(a) 0.12 kV

(b) 0.48 kV

Figure 2.4: Typical low voltage clusters.

2.4.2 Medium voltage

Figure 2.5a and 2.5b show us typical 7.2 kV and 12.49 kV clusters. Both examples are only composed of a majority of transformer gates, corresponding to connections with lower voltage levels. This, again, illustrates the purpose of the medium voltage. We clearly see that it spans over large areas in order to be as close as possible to the customers.

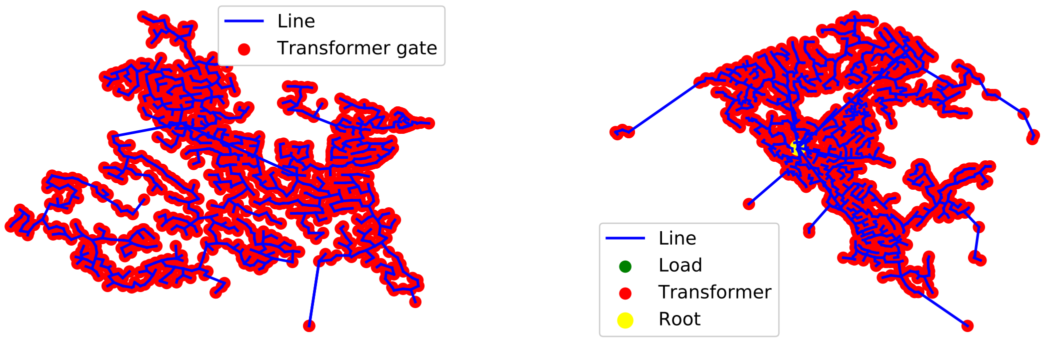

(a) 7.2 kV   (b) 12.47 kV

Figure 2.5: Typical medium voltage clusters.

The alert reader might have seen that the 7.2 kV example has no visible root node. As explained before, no transformer information was provided which would allow us to identify the root of the cluster. This issue has been bypassed using the ampacity and number of phases of the lines. The ampacity is defined as the maximum current, in amperes, that a conductor can carry continuously under the conditions of use without exceeding its temperature rating. A phase is defined as a unique wire connecting two nodes. A distinction is thus made between mono phased lines and three phased lines respectively corresponding to one line and three lines connecting two electrical buses. This implies that lines closer to the root of the network will have high ampacity and be three phased as they have to carry more power and thus more current. Figure 2.6 shows the network in Figure 2.5a with its identified root node and the high ampacity three phase lines of the network.

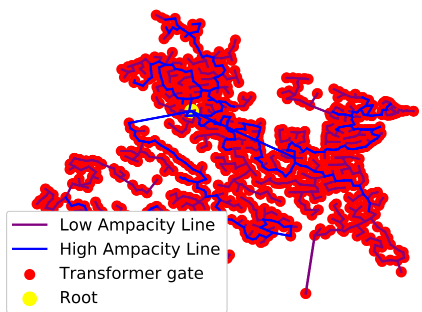

Figure 2.6: 7.2 kV example of Figure 2.5a with ampacity of lines.

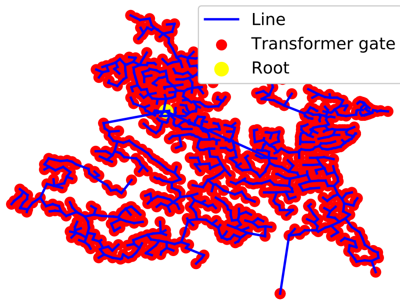

Figure 2.7: Maximum spanning tree of the 7.2 kV example in Figure 2.5a.

Also it may have been remarked that both examples in Figure 2.5 contain cycles, thus contradicting the radial assumption of the distribution system. This phenomenon is especially present in larger medium voltage clusters. Knowing that the radial structure is often considered as an assumption for distribution system optimization models it becomes interesting to modify the initial structure of the network in order to make it radial without modifying it's core structure.

This has been done using Prim's minimum spanning tree algorithm [19] which can be found in Appendix A.2. Suppose we have a graph $G = (V, E)$ then the minimum spanning tree of a graph $H = (V, A)$ is defined as the subgraph without cycles spanning over the entire node set V with the smallest sum of the edge weights. As the ampacity indicates where the electricity is supposed to be flowing with large magnitudes it is relevant to compute the maximum spanning tree of the voltage cluster where the edge weights correspond to the number of phases of the line times the ampacity. This means we will be selecting the high ampacity three phase lines before the other lines types thus keeping the core structure of the network. Prim's algorithm can be easily transformed into a maximum spanning tree algorithm giving us Figure 2.7. Note that we have only applied the algorithm on the 7.2 kV instance as we are only interested in generating these types of networks. The same reasoning can of course be applied to the 12.47 kV clusters.

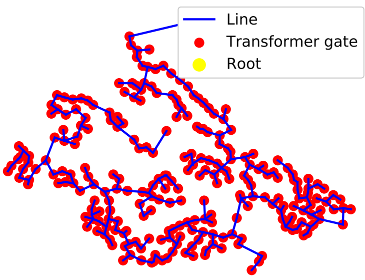

(a) 260 node branch

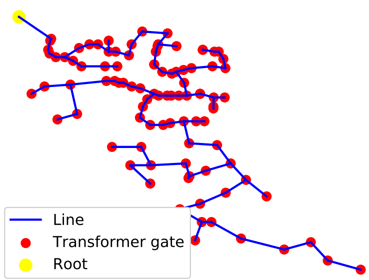

(b) 101 node branch

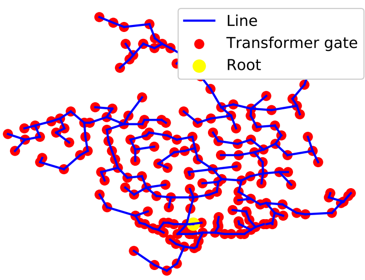

(c) 206 node branch

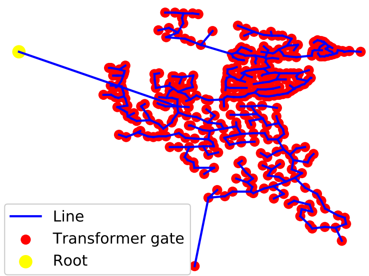

(d) 391 node branch

Figure 2.8: Branches of the 7.2 kV cluster example in Figure 2.7.

Having identified the root and removed the cycles of the clusters it now becomes interesting to have a look at each individual branches leaving the root node in Figure 2.7. These branches correspond to the medium voltage part of the independent feeders and are displayed in Figure 2.8.

2.4.3 Final instance

Suppose now that we would like to generate a typical feeder of a distribution system using the MV template from Figure 2.8b. This means we would have to stitch low voltage clusters to each individual transformer of the MV part of the feeder. We do this using the extracted LV templates from Appendix A.3. By stitching one randomly sampled LV template to each transformer we are able to generate network structures such as Figure 2.9. One can note that we dropped the geographical placement of the buses as we are stitching parts together that are not geographically related. It thus becomes more interesting to show the tree structure of the created network.

This network can now for example be used to compare different optimal dispatch algorithms designed for distribution systems.

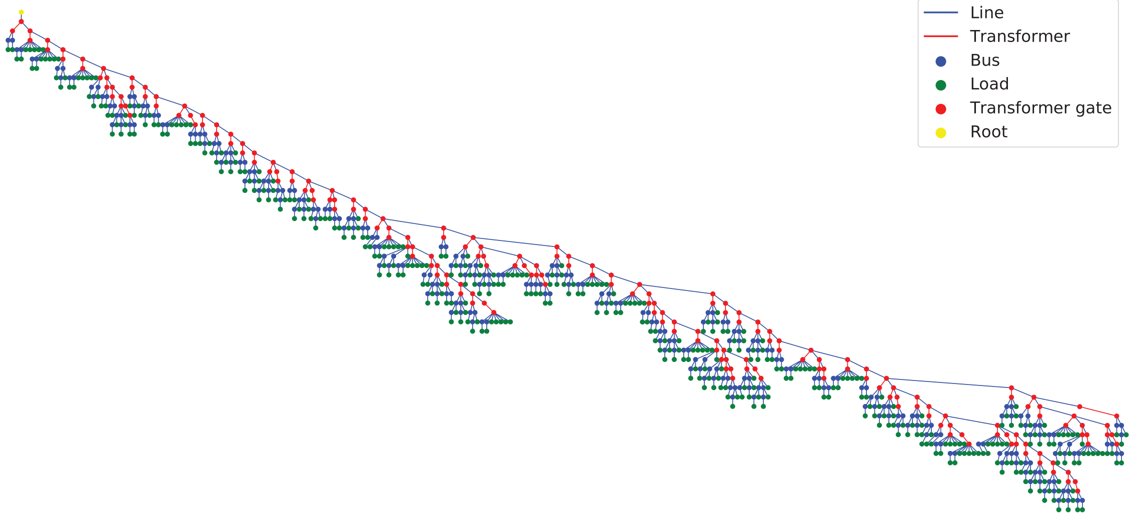

Figure 2.9: Feeder created by stitching typical LV clusters to the transformers of one typical MV voltage branch.

Chapter 3

Design of distribution systems: a new framework

The installation of PV systems has been investigated from the point of views of economical efficiency [12] and influence on distribution networks [20]. This is why it becomes interesting to study how to design distribution systems in order to cope with the presence of PV systems in LV clusters. A new framework is presented for designing and studying LV parts of distribution networks given a number of customers willing to install PV panels. The assumption will be made that customers and retailers work together in order to maximize the total welfare of the system which is not the case in reality. The amount of battery capacity and line capacity will be decided in order to cope with the demand and store excess PV production. At first this framework will be presented and explained. Then, an optimization model will be deduced based on the assumptions made in the previous sections and tested on a realistic test case. Finally, results will be discussed and conclusions will be drawn.

3.1 Framework

We create a model based on the typical structure of distribution systems representing the interaction between the different actors involved. It is composed of three nodes as shown in Figure 3.1. Nodes 1 and 2 (leaf nodes) correspond to low voltage clusters thus representing an aggregate of consumers. These nodes posses the following features and must satisfy the following constraints:

- They both have a BESS which can be charged and discharged according to the user's will.
- They both have a set of PV systems which produce power depending on the outside weather. Combining batteries with PV systems allows us to understand the optimal behavior of customers possessing these infrastructures as a response to pricing methods. Also, it will show us how the batteries can be optimally used in order to minimize the production costs of the entire system.

- They can withdraw/send infinite power from/to the grid.

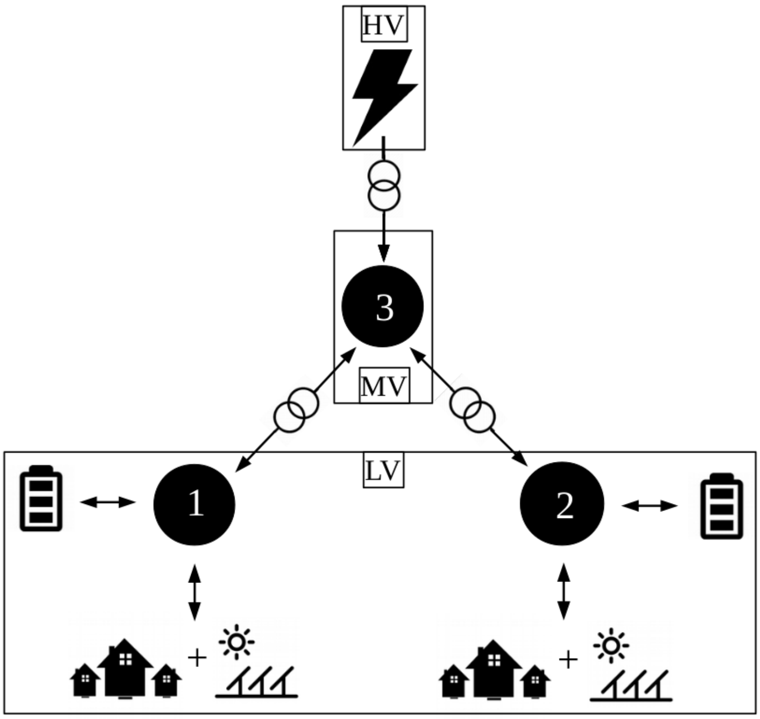

Figure 3.1: Schematic of the considered framework.

As both nodes correspond to LV clusters it becomes important to note that the logistical parameters such as the capacity of the batteries for example are not necessary the same for both systems.

Node three (root node) corresponds to the primary distribution connected to the transmission lines via the distribution substation. The actors controlling this node are the distribution system retailers as well as the DSO of the system.With this assumption, we can study the influence of interface prices on the congestion of the electrical lines. It will also show us later that both actors will have to work closely together in the future. The root node has the following features and constraints based on the duties of retailers and DSO's:

- It is connected to the transmission lines via the distribution substation.
- It has to satisfy the demand of the leaf nodes or pay a high price also known as the value of lost loads.
- It can choose the price of energy sold to the leaf nodes.
- It has to make sure that the capacity of the lines is never exceeded.

A final important assumption made is the fact that root node and leaf nodes work together in order to maximize the total welfare. In reality, this is not true as customers and retailers obviously want to maximize their own profit.

3.2 Infrastructures

Writing optimization models for the use and installation of technological infrastructures requires minimum knowledge about the technical and behavioral aspects of these installations. Two main first stage decisions have to be made corresponding to the BESS and maximal power flow allowed between root and leaf node.

Capacity and charge/discharge rate are the two only parameters which are chosen when designing the BESS. The system has three main components which will have to be adapted to the chosen parameters. The most obvious one is the battery module itself, it is the physical infrastructure that will store chemical energy. Next, a BESS converter is needed to convert the chemical energy stored in the battery to electrical energy. Finally, the balance of plant of the BESS stands for everything left related to the installation of the battery such as, for example, the wiring and switches of the system. The C-rate of a BESS corresponds to the ratio between charge/discharge rate and battery capacity. This C-rate depends on the type of battery technology considered and will have to be taken into account when designing the system.

Next, the line capacity of the LV system has to be decided. Two components have to be designed when setting up a low voltage network. The step down transformer connecting the LV network to the cluster serves as a first component. Indeed, different transformer models are available depending on the required nominal power of the module. Then, the capacity of the lines connecting the step down transformer to the individual customers has to be determined. It is important to note that approximating low voltage clusters by one node forces us to consider a fixed capacity on the flow between root and leaf node while this is not necessarily the case in reality. This maximal flow is thus the only parameter that has to be decided for the LV cluster.

3.3 Finding the optimal design

In order to design the optimal network connecting the medium voltage to the low voltage individual customers it becomes interesting to write an optimization problem to minimize the production cost and investment cost. The number of households and PV systems of each LV clusters is supposed to be fixed. The line capacity and battery storage of each leaf node are seen as decisions. We define L as the set of leaf nodes of the model. In our case L will be equal to $\{1, 2\}$ as we are only considering two leaf nodes. We define I as the set of infrastructures that can be installed, such that

$$I = \left\{\text{line capacity, battery energy capacity, battery charge/discharge rate}\right\}.$$

It has been decided that a perfect foresight model similar to Model 2 will be used. This approach has already been successful for similar problems in the past [21]. The idea here is to create a perfect foresight model where the first stage decisions correspond to the installed capacities of all technologies.

3.3.1 Objective

The objective of the optimization problem is

$$\min \quad \sum_{i\in I}\sum_{l\in L}\left(\mathrm{A}(\mathrm{IC}_i,\mathrm{LT}_i)\cdot v_{l,i}\right) + \sum_{s\in S}\frac{\Delta t}{|S|}\sum_{t\in T}\left(\mathrm{TC}(p_t^s) + \sum_{l\in L}\mathrm{VOLL}\cdot ls_{l,t}^s\right).$$

Parameter IC_i corresponds to the investment cost of component i in I. It is also called the overnight cost which refers to the fact that this cost is paid initially when setting up the installation and is thus not influenced by its usage. Parameter LT_i corresponds to the lifetime of component i. Function $\mathrm{A} : (\mathbb{R}_+,\mathbb{R}_+) \to \mathbb{R}_+$ represents the fixed daily equivalent cost formula, given daily discounting, and is defined as

$$\mathrm{A}(\mathrm{IC}_i,\mathrm{LT}_i) = \frac{\mathrm{IC}_i\cdot r}{1-\frac{1}{(1+r)^{\mathrm{LT}_i}}},$$

where r represents the discount rate. The fixed daily equivalent cost is a lump sum that needs to be paid daily for having one unit of a certain technology available [1]. Variable $v_{l,i}$ corresponds to the number of units of technology i which is installed in leaf node l. It has been chosen to use a general variable $v_{l,i}$ in order to reduce unnecessary mathematical notation. However, in the extensive form of the optimization problem these variables will be replaced by their real notation defined in the subsequent sections. Variable p_t^s represents the amount of power in kW withdrawn from the transmission lines by the root node during times step t of sampled scenario s. Variable $ls_{l,t}^s$ represents the amount of load which is shed[1] in leaf node l during times step t of sampled scenario s. Function $\mathrm{TC}(p_t^s) : \mathbb{R}_+ \to \mathbb{R}_+$ represents the total cost of withdrawing p_t^s from the transmission lines. Parameter VOLL is the value of lost loads and stands for the value per kW of not serving a customer.

It is also important to note that the objective function corresponds to the annuity of the system. The annuity of the system represents the daily cash flow required for setting up, powering, managing and operating two new low voltage clusters. No management and operating cost has been included in the objective due to the fact that these are less influenced

[1] Load shedding stands for not serving the demand in one of the leaf nodes. This demand has a certain cost, often denoted by the value of lost loads.

by the design decisions. The objective is therefore divided in two parts. The first component corresponds to the installed units of technology in both nodes. While the second component stands for the cost of managing power optimally throughout a set of sampled days. One can note that in a perfect foresight point of view the installed capacity can be considered as first stage decisions whereas the optimal management of the system corresponds to the next time stage decisions.

3.3.2 Constraints

Battery Energy Storage System

The energy tank model is adopted for the batteries, yielding the following constraint:

$$x^s_{l,t} = x^s_{l,t-1} + \Delta t \eta bc^s_{l,t-1} - \Delta t \frac{bd^s_{l,t-1}}{\mu} \quad \forall l \in L, \forall t \in T \setminus \{0\}, \forall s \in S,$$

where $x^s_{l,t}$ represents to the energy available expressed in kWh in the battery of leaf node l during time step t of scenario s, $bc^s_{l,t}$ and $bd^s_{l,t}$ respectively represent the battery charge and discharge rate expressed in kW of the battery in leaf node l during time step t of scenario s. Parameter Δt stands for the interval between two time steps and is expressed in hours. Parameters μ and η define the battery charge and discharge efficiency, they are both elements of $[0,1]$. We impose an empty tank at the start and end of the considered horizon

$$\begin{aligned} 0 &= x^s_{l,H} + \Delta t \eta bc^s_{l,H} - \Delta t \frac{bd^s_{l,H}}{\mu} \quad \forall l \in L, \forall s \in S, \\ 0 &= x^s_{l,0} \quad \forall l \in L, \forall s \in S. \end{aligned}$$

The bounds on the BESS variables are defined by the installed capacities,

$$\begin{aligned} 0 \le bc^s_{l,t} \le \mathrm{R}_l \quad \forall l \in L, \forall t \in T, \forall s \in S, \\ 0 \le bd^s_{l,t} \le \mathrm{R}_l \quad \forall l \in L, \forall t \in T, \forall s \in S, \\ 0 \le x^s_{l,t} \le \mathrm{C}_l \quad \forall l \in L, \forall t \in T, \forall s \in S, \end{aligned}$$

where R_l corresponds to the maximal charge rate of the battery in leaf node l thus replacing previously declared variable $v_{l,\text{battery charge rate}}$ and C_l represents the capacity installed in leaf node n and thus replaces variable $v_{l,\text{battery energy capacity}}$. We add constraint

$$\kappa \mathrm{C}_l = \mathrm{R}_l \quad \forall l \in L,$$

knowing that the C-rate of batteries links the capacity of the batteries to the maximal charge/discharge. Where κ is the C-rate of the considered battery type.

Power Flow

Optimal Power Flow (PF) has been regarded as one of the most important problems in power systems. We opt for the DC linear model approximation of power flow. Other models would represent overkill for the considered purpose. Indeed, the system approximates electrical buses by aggregating nodes. The other, more complicated, optimal power flow models are thus unnecessary. By using Figure 3.1 and the definition of flow through a network we get the following constraint for the PF at the root node:

$$\sum_{l \in L} f^s_{l,t} = p^s_t \quad \forall t \in T, \forall s \in S.$$

where $f^s_{l,t}$ is defined as the flow sent from the root node to leaf node l, during time step t of scenario s. The same reasoning can be applied to the leaf nodes, giving us

$$\mathrm{D}_{l,t} + bc^s_{l,t} + ps^s_{l,t} = f^s_{l,t} + bd^s_{l,t} + ls^s_{l,t} + \mathrm{Sys}_l \mathrm{RP}^s_{l,t} \quad \forall l \in L, \forall t \in T, \forall s \in S,$$

parameters $\mathrm{D}_{l,t}$ and $\mathrm{RP}^s_{l,t}$ respectively represent the the deterministic demand in leaf node l and the renewable power output of one PV system in time step t of scenario s. The demand of the leaf nodes is deterministic while the PV power output is chosen to be stochastic. Parameter Sys_l stands for the amount of PV systems installed in leaf node l. Variable $ps^s_{l,t}$ stands for the excess power thrown away in leaf node l and is called power shedding variable. Finally, by considering the bounds induced by the positivity and design decisions of each technology, we get that

$$\begin{aligned}
0 &\leq p^s_t \quad \forall t \in T, \forall s \in S, \\
0 &\leq ps^s_{l,t} \quad \forall l \in L, \forall t \in T, \forall s \in S, \\
0 &\leq ls^s_{l,t} \leq \mathrm{D}_{l,t} \quad \forall l \in L, \forall t \in T, \forall s \in S, \\
-\mathrm{F}_l &\leq f^s_{l,t} \leq \mathrm{F}_l \quad \forall l \in L, \forall t \in T, \forall s \in S.
\end{aligned}$$

The variable F_l represents the amount of line capacity connecting leaf node l and the root node. It replaces variable $v_{l,\text{line capacity}}$.

3.3.3 Final model

For the sake of clarity we put all constraints together, giving us Model 5. A list of the entire nomenclature can be found in Appendix B.1.

Model 5: Optimal design of low voltage networks.

$$
\begin{aligned}
\underset{\substack{p,ps,ls,f,bc,\\ bd,x,C_l,R_l,F_l}}{\text{minimize}} \quad & \sum_{i\in I}\sum_{l\in L}\Big(\mathrm{A}(\mathrm{IC}_i,\mathrm{LT}_i)\cdot v_{l,i}\Big)+\sum_{s\in S}\frac{\Delta t}{|S|}\sum_{t\in T}\Big(\mathrm{TC}(p^s_t)+\sum_{l\in L}\mathrm{VOLL}\cdot ls^s_{l,t}\Big) \\
\text{subject to} \quad & x^s_{l,t}=x^s_{l,t-1}+\Delta t\eta bc^s_{l,t-1}-\Delta t\frac{bd^s_{l,t-1}}{\mu}, && l\in L, t\in T\setminus\{0\}, s\in S,\\
& 0=x^s_{l,H}+\Delta t\eta bc^s_{l,H}-\Delta t\frac{bd^s_{l,H}}{\mu}, && l\in L, s\in S,\\
& 0=x^s_{l,0}, && l\in L, s\in S,\\
& \kappa \mathrm{C}_l=\mathrm{R}_l, && l\in L,\\
& 0\le bc^s_{l,t}, && l\in L, t\in T, s\in S,\\
& 0\le bd^s_{l,t}, && l\in L, t\in T, s\in S,\\
& 0\le x^s_{l,t}, && l\in L, t\in T, s\in S,\\
& bc^s_{l,t}\le \mathrm{R}_l, && l\in L, t\in T, s\in S,\\
& bd^s_{l,t}\le \mathrm{R}_l, && l\in L, t\in T, s\in S,\\
& x^s_{l,t}\le \mathrm{C}_l, && l\in L, t\in T, s\in S,\\
& \sum_{l\in L} f^s_{l,t},=p^s_t, && t\in T, s\in S,\\
& \mathrm{D}_{l,t}+bc^s_{l,t}+ps^s_{l,t},=f^s_{l,t}+bd^s_{l,t}+ls^s_{l,t}+\mathrm{Sys}_l\mathrm{RP}^s_{l,t}, && l\in L, t\in T, s\in S,\\
& 0\le p^s_t, && t\in T, s\in S,\\
& 0\le ps^s_{l,t}, && l\in L, t\in T, s\in S,\\
& 0\le ls^s_{l,t}, && l\in L, t\in T, s\in S,\\
& ls^s_{l,t}\le \mathrm{D}_{l,t}, && l\in L, t\in T, s\in S,\\
& -\mathrm{F}_l\le f^s_{l,t}, && l\in L, t\in T, s\in S,\\
& f^s_{l,t}\le \mathrm{F}_l, && l\in L, t\in T, s\in S
\end{aligned}
$$

This model is convex as we only have linear constraints and $\mathrm{TC}(p^s_t)$ is designed in order to be convex. This means that every local optimum will be a global optimum [22] allowing us to rely on standard solvers used for these types of models.

3.4 Test case

We now test our model for some parameter values and study the results in order to determine what should be the optimal design of the system.

3.4.1 Computational characteristics

The computational parameters of the implementation can be found in Table 3.1 and have been chosen in order to have reasonable computation time while keeping a high detailed version of the problem.

Δt	H	$\max_t \lvert\Omega_t\rvert$	$\lvert S\rvert$
15 minutes	95	10	6000

Table 3.1: Computational characteristics.

3.4.2 Leaf node characteristics

The characteristics of the leaf nodes are shown in Table 3.2 and have been chosen based on the results of Section 2.3.1. The deterministic demand has been generated using aggre-

Node	Households	Total line length	PV systems	μ	η	κ
1	10	1 km	2	0.9	0.9	2
2	15	1.5 km	3	0.9	0.9	2

Table 3.2: Characteristics of the leaf nodes.

gates of daily demand profiles of the model described in [23]. This model generates high resolution demand data and is based upon a combination of patterns of active occupancy (i.e.when people are at home and awake), and daily activity profiles that characterize how people spend their time performing certain activities. The model generates typical demand profiles given a month and a number of occupants. In this case the demand profiles have been generated for the month of November and Table 3.3 provides the number of households for each occupancy level in the leaf nodes. The created profiles have been displayed in

Occupants	1	2	3	4	5	Total
Households in node 1	1	2	4	2	1	10
Households in node 2	2	3	5	3	2	15

Table 3.3: Number of households for each occupancy level.

Figure 3.2. The initial one minute interval data has been transformed in 15 minute interval data by computing the average value of 15 consequent time steps .

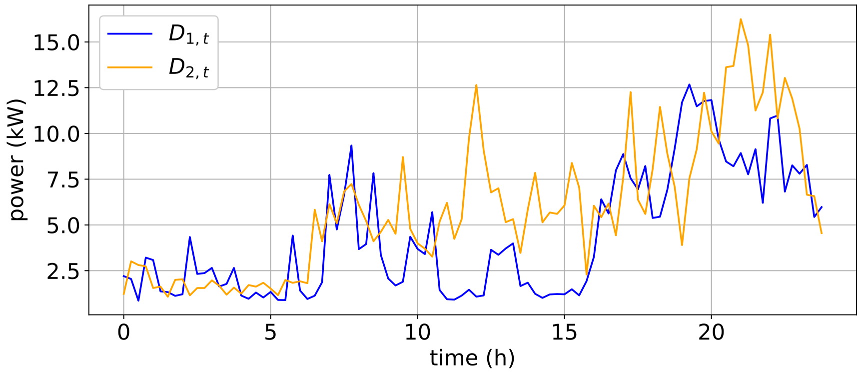

Figure 3.2: Demand profiles of the leaf nodes in the experimental setup.

The lattice of uncertainty defining the PV output has been created using [24] which provides a chronological probability model of photo voltaic generation on the basis of conditional probability and non-parametric kernel density estimation. This model perfectly adjusts for the lattice model of uncertainty as it computes the conditional probability density function between adjacent time steps. Generating these conditional probability density functions requires initial data in order to compute the required parameters. The California Solar Initiative, a solar rebate program for Californian electricity consumers, provides simulated solar data for a set of approximately five hundred CSI PV installations [25]. This data covers 5 years of 15 minute interval PV output data. A specific system called PGE-SASH-4101 located in San Jose, California has been chosen among all systems.

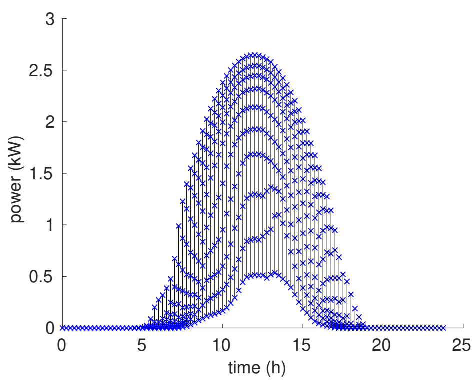

Figure 3.3: Lattice nodes generated for the lattice model.

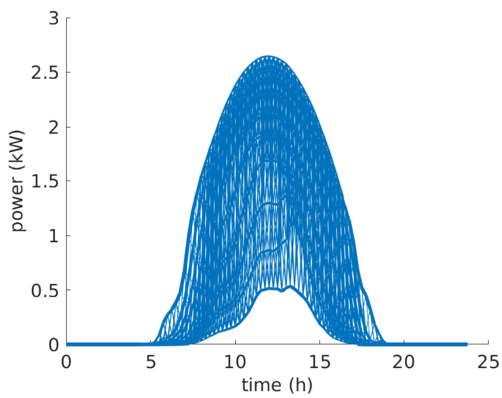

Figure 3.4: Set of 20000 samples generated by the scenario generator using the lattice model.

California is known to be one of the most sunny areas in the United States and thus fits perfectly for our case study. Indeed, as we are looking for high PV penetration this PV system will perfectly fit our needs. It has a peak output of 3 kW corresponding to a typical household PV system. For the sake of computational simplicity it will be supposed that the PV output of all PV systems is the same regardless of the leaf node associated to it. This is justified by the assumption that both leaf nodes correspond to adjacent LV clusters implying that the PV output should be highly correlated between two systems. Each node of the lattice will thus represent a common power output for all PV systems. Figure 3.3 and 3.4 respectively show the nodes of the lattice for each time step and a set of PV output samples generated by the model.

3.4.3 Costs

As explained before, the objective function is composed of two parts. The parameters of the second part, corresponding to the design of the network, can be found in Table 3.4. The first part parameters, coming from the design decisions of the system, can be found

Parameter	$\mathrm{MC}(p_t^s)$	$\mathrm{TC}(p_t^s)$	VOLL
Value	$0.008 p_t^s \frac{€}{\mathrm{kWh}}$	$0.004 (p_t^s)^2 \frac{€}{\mathrm{h}}$	$8.3 \frac{€}{\mathrm{kWh}}$

Table 3.4: Costs related to the management of the network.

in Table 3.5. The BESS parameters have been taken from [10] and have been obtained by private communication with companies working in the sector. The LV cluster parameters are computed using available information in [9].

BESS			
Component	Module	Converter	BoP
IC_i	$270 \frac{€}{\mathrm{kWh}}$	$80 \frac{€}{\mathrm{kW}}$	$200 \frac{€}{\mathrm{kWh}}$
LT_i	15 years	20 years	20 years
$\mathrm{A}(\mathrm{IC}_i, \mathrm{LT}_i)$	$0.06955 \frac{€}{\mathrm{kWh\ day}}$	$0.01716 \frac{€}{\mathrm{kW\ day}}$	$0.04291 \frac{€}{\mathrm{kWh\ day}}$

LV cluster		
Component	Lines	Transformer
IC_i	$800 \frac{€}{\mathrm{kW\ km}}$	$189 \frac{€}{\mathrm{kW}}$
LT_i	25 years	25 years
$\mathrm{A}(\mathrm{IC}_i, \mathrm{LT}_i)$	$0.15176 \frac{€}{\mathrm{kW\ km\ day}}$	$0.03585 \frac{€}{\mathrm{kW\ day}}$

Table 3.5: Investment cost, lifetime and fixed daily equivalent cost of the considered technologies.

One can note that the fixed daily equivalent investment cost of constructing low voltage cluster line capacity is higher compared to the fixed daily equivalent investment cost of constructing a BESS. This will influence the optimal design decisions and should thus be kept in mind when reading the subsequent sections.

3.5 Results

The implementation has been made using programming language `AMPL` and is solved using the `Gurobi` solver with the default barrier algorithm. The used computer has an Intel(R) Core(TM) i7-8550U CPU with eight threads at 1.80GHz and 16Gb of RAM memory. The `_solve_time` is equal to 837.88 s while the `_ampl_time` is equal to 49.68 s, they respectively represent the time needed to solve the model and the preparation time needed to set up the model. As this model has been created in order to design systems it means that it will have to be run only once to get the optimal first stage decisions, implying that more samples could have been generated during the set up. However, increasing the size of S would result in memory errors an is due to the fact that a 15 minute interval has been chosen between subsequent time steps. The first stage decisions are shown in Table 3.6.

Leaf node	F	C	R
1	7.5503 kW	10.2514 kWh	5.1257 kW
2	8.12091 kW	17.3315 kWh	8.66576 kW

Table 3.6: Optimal first stage decision variables of Model 5 with the test case of Section 3.4.

3.5.1 Interpretation

The decision variables define a network composed of positive line capacity and positive battery capacity that never needs to shed load. A first intuition is to think that battery capacity has been created to store the excess PV output.

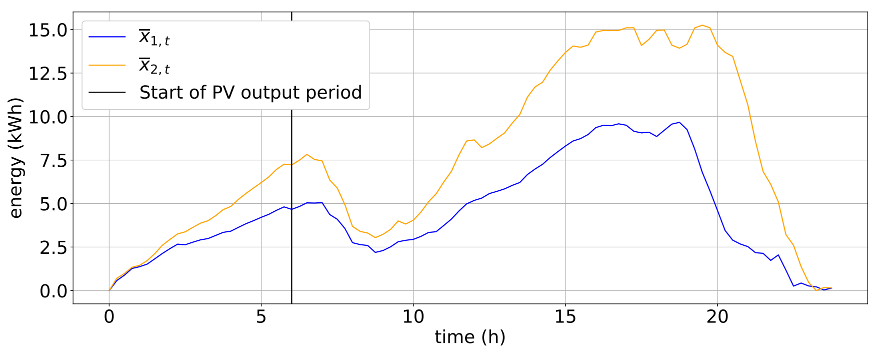

Figure 3.5: Average energy stored in the battery when using Model 5. Two charging periods can be identified.

This is indeed true but it is not the only explanation for high battery investment. As noted previously, we have seen that the annualized investment cost of BESS is lower than the annualized investment cost of LV cluster capacity thus resulting in the fact that BESS investment will be prioritized. Using Figure 3.5 we see that the storage facility is filled during the first six hours of the day. No PV production can be measured at that period. This can be explained by the fact that as batteries have lower investment cost it is interesting to use them in order to reduce line capacity. Indeed, having more storage capacity than needed allows the user to smooth his downwards flow throughout the day and thus reduce his peak demand. This is confirmed by Figure 3.6, which shows that during periods of low demand excess flow is sent to the leaf nodes while during periods of high demand the flow often equalizes the maximal built capacity and has a lower value compared to the demand curve.

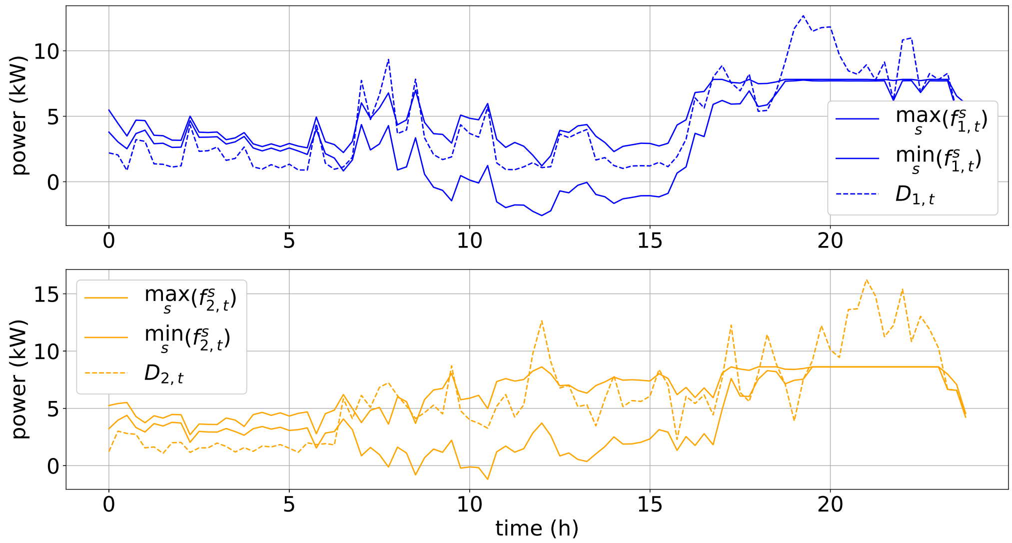

Figure 3.6: Comparison between demand, maximal flow and minimal flow for both leaf nodes over time. From 0 to 5 am $f^s_{l,t}$ is always greater or equal to $D_{l,t}$.

When looking at the average battery energy in Figure 3.5 we see that two periods can be identified. The first one corresponds to the period from 0 am to 8 am. The battery is filled during the first six hours before demand starts to increase in node one. This high demand is then satisfied using the stored energy of the battery in addition with the PV supply if the weather conditions allow it. During the second period, from 9 am to 12 pm, we see that the battery is again charged until 5 pm and discharged during the peak power period going from 8 pm to 12 pm. The battery thus serves as a way to anticipate higher demand.

Finally, by imposing that no power can be provided using transmission lines (i.e. $p^s_t = 0$ for all t in T and for all s in S) we get the results of Table 3.7. One can observe that less BESS capacity has been created because it cannot be used any more to smooth the flow between root node and leaf node and confirms our inference. Also, it can be seen that line capacity will still be needed. This can be explained by the fact that investing in line capacity allows the leaf nodes to exchange power thus reducing the production cost.

Leaf node	F	C	R
1	3.251 kW	8.773 kWh	4.335 kW
2	3.251 kW	8.819 kWh	4.476 kW

Table 3.7: Optimal first stage decision variables when $p_t^s = 0$ for all t in T and for all s in S.

Chapter 4

Influence of retail pricing on customers and network congestion

In Chapter 3 the network has been designed in order to maximize the system welfare. However, this cannot be easily applied in reality. Customers, DSO's and retailers do not usually work together, implying that new assumptions will have to be made. The initial framework of Chapter 3 is kept but assumptions are modified.

In this chapter, we consider that each node now makes his decisions individually. This means that the leaf nodes will have to decide whether to charge or discharge their batteries and whether to sell or buy electricity from the root node in order to minimize their payment while the root node will have to choose the way it prices electricity in order to maximize its own profit. This chapter will thus compute and study the optimal reaction of the customers in the created network to different pricing methods which are currently applied in distribution systems or have been proposed as alternatives. This behavior will then be studied from a network point of view and conclusions will be drawn regarding the congestion of the network.

4.1 Assumptions

We consider the same framework as depicted in Figure 3.1 but behavioral changes are assumed for the different actors involved and are summarized in Figure 4.1 The root node now decides the interface price knowing that it has to manage the system and thus make sure that the line capacities are not exceeded. This price will influence the behavior of the customer thus indirectly influencing how electricity will have to be supplied and when it will have to be generated. The customer, on the other hand, manages his battery optimally in order to minimize his payment and thus maximize his profit. He thus does not care if the line capacities are exceeded. This will have to be kept in mind as in Chapter 3 we explained that battery capacity has been created in order to reduce line capacity.

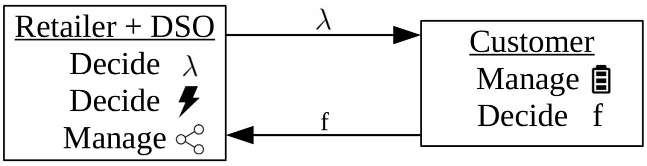

Figure 4.1: Schematic illustrating the behavior of the individual actors involved in the considered framework.

4.2 Available pricing methods

In Belgium, two pricing methods are available to customers. These pricing methods are called flat rate pricing and time of use (also called tarif bi-horaire) pricing.

4.2.1 Flat rate

Flat rate corresponds to the simplest form of pricing electricity, it simply computes the total amount of electricity consumed and multiplies it with a constant value that has been decided beforehand by the retailer. This price is available for the customer and his payment can thus be computed using

$$P_c = \Delta E \cdot \lambda,$$

where P_c corresponds to the customers payment, ΔE corresponds to the energy consumed during the considered interval (in kWh) and λ corresponds to the tariff price (in $\frac{€}{\text{kWh}}$). It should be noted that the payment can be reduced if the customer sends energy to the root node.

4.2.2 Time of use

On the other side, time of use pricing represent a way of pricing electricity which is time dependent. Two periods are identified for this pricing option. First, the peak period corresponding to a higher price during day time, often going from 8 am to 10 pm depending on the considered municipality. Secondly, the off peak period standing for the remaining night time period with a lower price. These prices are available for the customer and can thus be computed using

$$P_c = \Delta E_t \cdot \lambda_t,$$

where ΔE and λ are time dependent.

4.2.3 Optimization model

We create a stochastic optimization model used for computing the optimal management strategy for the leaf nodes. This model will help us understand the optimal behavior of the customer as a reaction to the imposed prices. The leaf node index notation has been dropped for the sake of clarity, giving us Model 6.

Model 6: Optimal leaf node behavior.

$$
\begin{aligned}
\underset{x,f,bc,bd}{\text{minimize}} \quad & \sum_{t\in T} \sum_{w_{[t]}\in\Omega_{[t]}} \mathbb{P}\big(w_{[t]}\big)\lambda_t \Delta t f_t^{w_{[t]}} \\
\text{subject to} \quad & x_t^{w_{[t]}} = x_{t-1}^{a(w_{[t]})} + \Delta t \eta bc_{t-1}^{a(w_{[t]})} - \Delta t \frac{bd_{l,t-1}^{a(w_{[t]})}}{\mu}, && t \in T\setminus\{0\}, w_{[t]} \in \Omega_{[t]}, \\
& 0 = x_H^{w_{[H]}} + \Delta t \eta bc_H^{w_{[H]}} - \Delta t \frac{bd_{l,H}^{w_{[H]}}}{\mu}, && w_{[H]} \in \Omega_{[H]}, \\
& 0 = x_0^{w_{[0]}}, && w_{[0]} \in \Omega_{[0]}, \\
& 0 \le bc_t^{w_{[t]}}, && t \in T, w_{[t]} \in \Omega_{[t]}, \\
& 0 \le bd_t^{w_{[t]}}, && t \in T, w_{[t]} \in \Omega_{[t]}, \\
& 0 \le x_t^{w_{[t]}}, && t \in T, w_{[t]} \in \Omega_{[t]}, \\
& bc_t^{w_{[t]}} \le \mathrm{R}, && t \in T, w_{[t]} \in \Omega_{[t]}, \\
& bd_t^{w_{[t]}} \le \mathrm{R}, && t \in T, w_{[t]} \in \Omega_{[t]}, \\
& x_t^{w_{[t]}} \le \mathrm{C}, && t \in T, w_{[t]} \in \Omega_{[t]}, \\
& \mathrm{D}_t + bc_t^{w_{[t]}} + ps_t^{w_{[t]}} = f_t^{w_{[t]}} + bd_t^{w_{[t]}} + \mathrm{Sys}_l \mathrm{RP}_t^{w_{[t]}}, && t \in T, w_{[t]} \in \Omega_{[t]}, \\
& 0 \le ps_t^{w_{[t]}}, && t \in T, w_{[t]} \in \Omega_{[t]}
\end{aligned}
$$

A stochastic optimization problem is proposed. The customer wants to minimize his expected cost over the considered time horizon. This model is very similar to Model 5 defined in Section 3.3.3. The objective changes, we lose the line capacity constraints as well as the power flow constraints at the root and the model is adapted in order to work with a scenario tree representation of uncertainty. This model is linear and can easily be solved using conventional solvers. Note that for flat rate pricing we have that $\lambda_{t_1} = \lambda_{t_2}$ for all t_1, t_2 in T.

4.3 Test case

A general test case is created to compare all pricing methods with each other. Smaller computational characteristics will be used, otherwise excessive computation times would be needed given that a stochastic model is chosen instead of the perfect foresight approach. Table 4.1 shows the considered computational characteristics of the test case. The deterministic demand data and PV production models of Section 3.4.2 have been kept. The demand profiles are the same as in Figure 3.2 but have been averaged over two hours instead of 15 minutes. The lattice model has also been adapted for the computational parameters of Table

Δt	H	$\max_t \lvert\Omega_t\rvert$	$\lvert S\rvert$
2 hours	11	5	50000

Table 4.1: Computational characteristics of the test case.

4.1. Both the new demand profiles and lattice model can be found in appendix C.1. The first stage decisions of Table 3.6 are now considered as parameters of the problem. Finally, λ_t is taken from [4] and can be found in Table 4.2. Parameter λ corresponds to the electricity price in $\frac{€}{\text{kWh}}$. Other parts also have to be added to the payment but are not dependent of the quantity of energy withdrawn and are thus not included.

Pricing method	Flat rate	Time of use
Peak	0.2672 $\frac{€}{\text{kWh}}$	0.2041 $\frac{€}{\text{kWh}}$
Off peak	0.2672 $\frac{€}{\text{kWh}}$	0.2833 $\frac{€}{\text{kWh}}$

Table 4.2: Electricity prices taken from [4].

4.4 Results

Both models have been tested using the test case of Section 4.3 and the same computer as in Chapter 3. Again, this has been implemented using programming language `AMPL` using the `Gurobi` solver with the default dual simplex algorithm. The computation times are given in Table 4.3.

	Node 1		Node 2	
Time	Flat rate	Time of use	Flat rate	Time of use
`_ampl_time`	12.05 s	10.22 s	12.04 s	11.56 s
`_solve_time`	12.90 s	11.81 s	15.15 s	15.64 s

Table 4.3: Computation times for solving Model 6 with the test case of Section 4.3.

4.4.1 Flat rate

In this case, the optimal behavior can be easily derived using logical reasoning. The battery efficiency hypothesis implies that more power needs to be transferred to store the same quantity of energy. Hence, it is more interesting for the consumer to sell immediately its excess supply to the root node. He will indeed be able to buy it back at the same price later, thus meaning he has not wasted any energy due to BESS efficiency losses. Further, he will never buy unnecessary power to anticipate possible high loads in subsequent time stages. The implementation confirms the results as the battery is never charged during any time step. By defining the net demand, with symbol $\mathrm{ND}_{l,t}^{w_t}$, as

$$\mathrm{ND}_{l,t}^{w_t} = \mathrm{D}_{l,t} - \mathrm{Sys}_l \mathrm{RP}_{l,t}^{w_t}$$

we are able to plot Figure 4.2. We see that the minimal and maximal flows entering each leaf node respectively equal the maximal and minimal net demand for each time step and each leaf node thus confirming our inference.

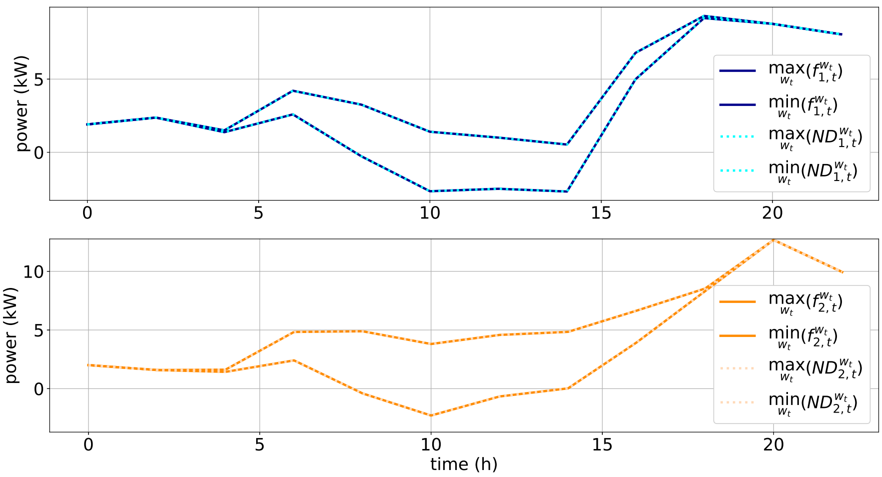

Figure 4.2: Comparison of the maximal and minimal flow going to the leaf node with maximal and minimal net demand for flat rate pricing.

Next, it is also interesting to have a look at how the behavior of both leaf nodes will influence the power withdrawn from the transmission lines and when power shedding at the root node will occur due to simultaneous upwards flow of both leaf nodes.

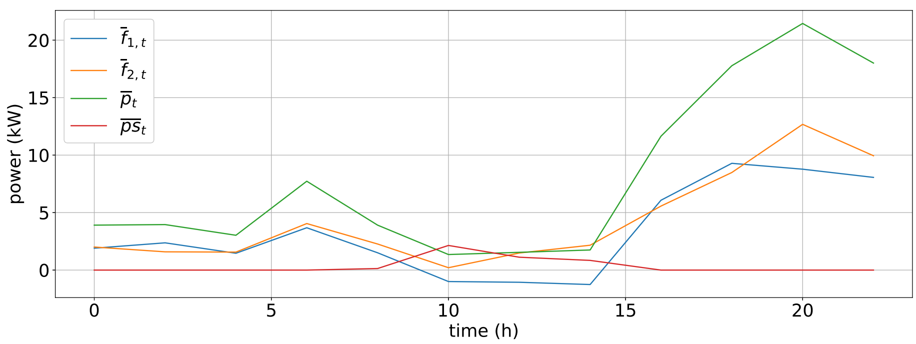

Figure 4.3: Average customer behavior and influence on the root node when using flat rate pricing.

This is shown in Figure 4.3. We are able to identify three periods. First, The demand is satisfied using only downwards flow until 8am. At this moment solar supply starts to appear, resulting in a lower average flow for both nodes and is due to the fact that both customers will automatically send power to the leaf node if their net demand is negative. This results in power shedding at the root node as no battery can be installed there. Finally, at 3pm as PV power production of both systems start to decrease and their demand starts to increase, the leaf nodes augment their downwards flow inducing high power production at the leaf nodes.

Some conclusions can thus be made regarding the behavior of customers reacting to flat rate pricing. First of all, batteries are not used and have thus been unnecessarily installed. Secondly, we see that for LV networks situated at small distances from each other, excess PV power output will be sent simultaneously to the grid. Finally, because of this behavior, demand at the start and end of the day will never be satisfied by eventual stored energy thus resulting in high simultaneous power withdrawal from transmission lines.

4.4.2 Time of use

Again, the optimal decisions can be easily deduced. As the price is lower during off peak hours it is more interesting to use electricity generated during that period. The customer will thus try to fill his battery throughout the morning before the peak period starts, then use this electricity during the day and sell the excess battery energy before the peak period starts. This means he will be able to use as much cheap energy as possible throughout the day. The battery profile of Figure 4.4 illustrates this, we clearly see that for both leaf nodes

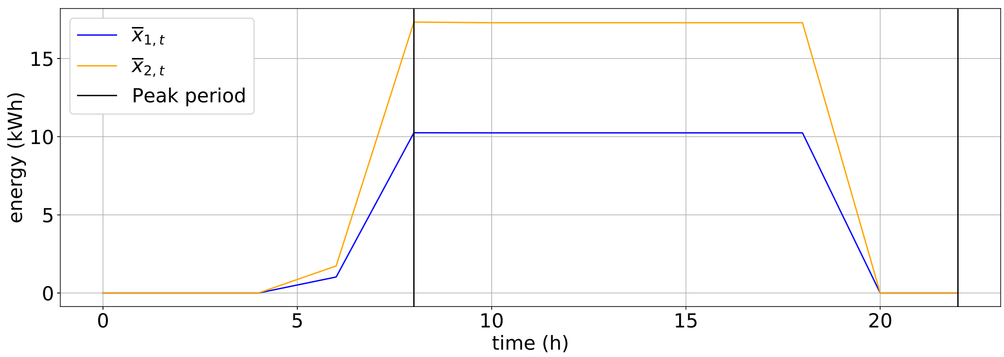

Figure 4.4: Average stored energy for both leaf nodes when using time of use pricing.

the battery is charged before the peak period and discharged during the peak period. The battery is nearly never discharged before 6 pm and the stored energy is thus always used to reduce the peak demand at that moment. This also implies that excess PV output will result in a negative flow leaving the leaf nodes as the batteries are both full. This can be seen in Figure 4.5 where power shedding appears only during the peak PV power output hours.

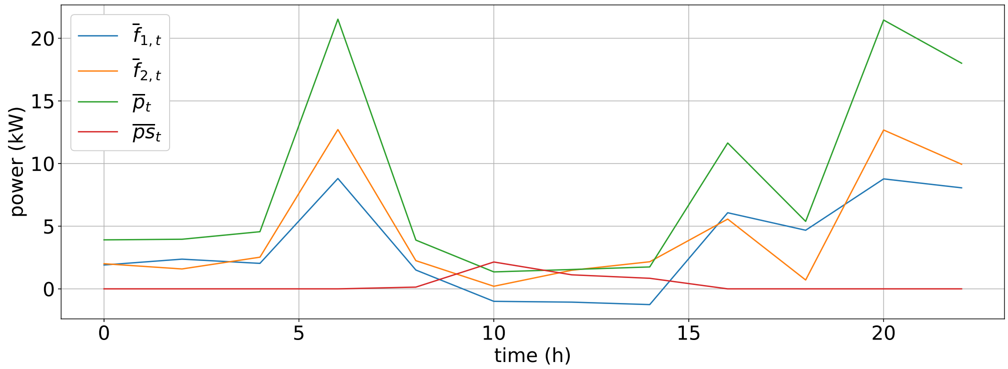

Figure 4.5: Average customer behavior and the influence on the root node when using time of use pricing.

With some reasoning it is possible to come up with a similar solution which will not change the payment of the customers and highly reduce the root node cost. Instead of charging and discharging the battery during only one time step it could be done throughout the entire period. We illustrate this using Figure 4.6. Knowing that the battery is always filled at 6am

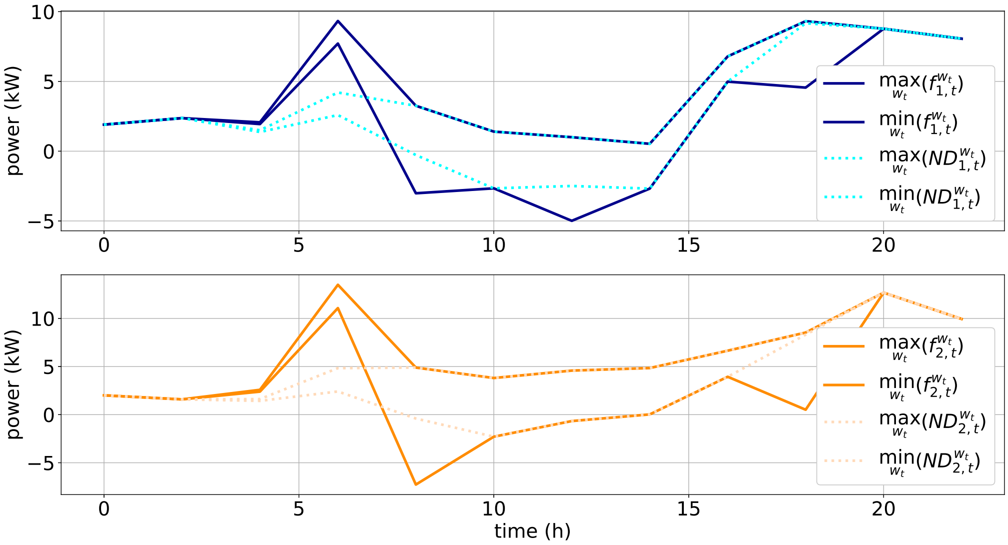

Figure 4.6: Comparison of the maximal and minimal flow going to the leaf node with maximal and minimal net demand for time of use pricing.

it is indeed possible to charge it equally from midnight until 6am thus reducing the peak downwards flow during that period. The same could also be done during the peak period of the day. Instead of entirely discharging the battery at 6 pm one could do this over the entire peak period again smoothing the demand over that period without changing the payment of the leaf nodes.

However, this does not change the fact that leaf nodes will never store excess PV power supply which can be explained by two facts. First of all, BESS efficiency losses reduce the energy quantity that can be sold. And secondly, the fact that the sell price is higher during the peak period.

A few conclusions can be drawn from the optimal behavior of customers when using time of use pricing. First of all, we see that the installed battery will only be used by the customer to store cheap energy in the battery. This energy mainly comes from complementary power withdrawn from transmission lines and minor excess PV power. Also, if more BESS capacity had been installed we would have seen that the battery would be used to reduce the payment of the customer. It would be filled during off peak hours and excess energy would be sold during peak hours thus reducing the customer's bill. Secondly, excess PV power will never be stored and always lead to upwards flow during the peak hours inducing simultaneous upward flow for geographically adjacent leaf nodes thus enhancing the risk of power shedding. Finally, time of use pricing will have the benefit of reducing overall loads during peak hours as the customers will prioritize discharging his battery to buying downwards flow from the root node.

4.4.3 Network influence

Let us first ask ourselves what a good pricing method is and what influence it should have on the flows going through the network. First of all, it should avoid congestion of the lines. As explained before we have reduced the line capacity and replaced it by battery capacity in order to reduce investment costs. This means that we might have a lot of congestion as the DSO does not choose what flow the leaf node will withdraw/inject. Next, we should have a look at the average production cost which tells us what the total cost of the system will be. Finally, one should pay attention to the consumer payment. This value represents how much the consumer will pay in average over one day if he follows the decisions of the optimization problem.

This analysis has been summarized in Table 4.4. Flat rate pricing has smaller average production cost and identical power shedding compared to time of use pricing. This is due to the behavior of the customer. Indeed, the behavior of time of use pricing customers makes it more likely for both nodes to buy electricity simultaneously because the battery is always charged during the first 6 hours of the day thus increasing simultaneous production. The production cost will however be smaller when the production is smooth over the considered horizon. This is due to the quadratic nature of function TC and thus explains why flat rate pricing has smaller production cost. The upwards flow of both nodes will behave similarly due to the efficiency losses of the BESS thus canceling out the benefit of being able to compensate the demand of one node with the renewable production of the other. This is why equal power shedding can be observed for both cases. Finally, the two pricing methods behave really bad when looking at the congestion percentage. However we see that the required capacity for both methods in order to remove congestion is not that far away from the values we computed for the design of the network.

Feature	Flat rate	Time of use
Leaf nodes		
Average payment of node 1	21.28 €	19.50 €
Average payment of node 2	27.79 €	25.94 €
Root node		
Average power shedding	8.48 kW	8.48 kW
Average power consumption	192.12 kWh	197.95 kWh
Average production cost	11.10 €	12.12 €
Lines		
Congestion % node 1	25.00 %	25.00 %
Congestion % node 2	25.00 %	25.01 %
F for 90 % prob. of uncongested line node 1	8.77 kW	8.77 kW
F for 90 % prob. of uncongested line node 2	9.94 kW	12.68 kW
F for 95 % prob. of uncongested line node 1	9.32 kW	9.23 kW
F for 95 % prob. of uncongested line node 2	12.68 kW	13.34 kW
F for 100 % prob. of uncongested line node 1	9.32 kW	9.33 kW
F for 100 % prob. of uncongested line node 2	12.68 kW	13.50 kW

Table 4.4: Network influence comparison between flat rate pricing and time of use pricing.

4.5 Alternatives

We have seen that flat rate pricing and time of use pricing are not optimized for the designed network, this is why it becomes interesting to start looking at alternative pricing methods. We will consider Real Time (RT) pricing and compare it with the Perfect Foresight (PF) policy. Real time pricing assigns a price for each possible scenario of the scenario tree. Comparing this pricing method with a perfect foresight model allows us to understand what the value of knowing the PV power output in advance represents for the problem.

4.5.1 Real time pricing and perfect foresight

The cost for the consumer for one time step in one scenario is

$$P_c = \Delta E_t^{w[t]} \cdot \lambda_t^{w[t]},$$

where ΔE and λ are time and scenario dependent. Real time pricing is in reality really difficult to apply as the customer has to be able to understand how he will be charged for consuming energy. This is quite contradictory with the concept of real time pricing. Giving him a price dependent on each scenario makes it way more complicated for him to plan his consumption.

4.5.2 Optimization problem

From an optimization point of view it comes that the distribution system interaction between customer and retailer can be seen as a competitive market. The optimal scenario prices and network flow decisions are thus obtained by considering the collaboration of both leaf nodes and the root node. It is thus sufficient to solve an adapted version of the economic dispatch problem presented in Section 1.2.2. The nodal interface prices will then be obtained using the dual multipliers of their respective power flow constraints.

Model 7: Optimal real time system decisions.

$$
\begin{aligned}
\underset{x,f,bc,bd,p}{\text{minimize}} \quad & \sum_{t\in T}\sum_{w_{[t]}\in\Omega_{[t]}} \mathbb{P}\big(w_{[t]}\big)\Delta t\Big(\mathrm{TC}\Big(p_t^{w_{[t]}}\Big)+\sum_{l\in L}\mathrm{VOLL}\ ls_{l,t}^{w_{[t]}}\Big) \\
\text{subject to} \quad & x_{l,t}^{w_{[t]}}+\Delta t\frac{bd_{l,t-1}^{a(w_{[t]})}}{\mu}=x_{l,t-1}^{a(w_{[t]})}+\Delta t\eta bc_{l,t-1}^{a(w_{[t]})}, && l\in L, t\in T\setminus\{0\}, w_{[t]}\in\Omega_{[t]}, \\
& \Delta t\frac{bd_{l,H}^{w_{[H]}}}{\mu}=x_{l,H}^{w_{[H]}}+\Delta t\eta bc_{l,H}^{w_{[H]}}, && l\in L, w_{[H]}\in\Omega_{[H]}, \\
& 0=x_{l,0}^{w_{[0]}}, && l\in L, w_{[0]}\in\Omega_{[0]}, \\
& 0\le bc_{l,t}^{w_{[t]}}, && l\in L, t\in T, w_{[t]}\in\Omega_{[t]}, \\
& 0\le bd_{l,t}^{w_{[t]}}, && l\in L, t\in T, w_{[t]}\in\Omega_{[t]}, \\
& 0\le x_{l,t}^{w_{[t]}}, && l\in L, t\in T, w_{[t]}\in\Omega_{[t]}, \\
& bc_{l,t}^{w_{[t]}}\le \mathrm{R}_l, && l\in L, t\in T, w_{[t]}\in\Omega_{[t]}, \\
& bd_{l,t}^{w_{[t]}}\le \mathrm{R}_l, && l\in L, t\in T, w_{[t]}\in\Omega_{[t]}, \\
& x_{l,t}^{w_{[t]}}\le \mathrm{C}_l, && l\in L, t\in T, w_{[t]}\in\Omega_{[t]}, \\
& \mathrm{D}_{l,t}+bc_{l,t}^{w_{[t]}}+ps_{l,t}^{w_{[t]}}=f_{l,t}^{w_{[t]}}+bd_{l,t}^{w_{[t]}}+\mathrm{Sys}_l\mathrm{RP}_t^{w_{[t]}}, && l\in L, t\in T, w_{[t]}\in\Omega_{[t]}, \\
& \sum_{l\in L} f_{l,t}^{w_{[t]}}=p_t^{w_{[t]}}, && t\in T, w_{[t]}\in\Omega_{[t]}, \\
& -\mathrm{F}_l\le f_{l,t}^{w_{[t]}}, && l\in L, t\in T, w_{[t]}\in\Omega_{[t]}, \\
& f_{l,t}^{w_{[t]}}\le \mathrm{F}_l, && l\in L, t\in T, w_{[t]}\in\Omega_{[t]}
\end{aligned}
$$

This model is very similar to the Model 5, one can note that the objective has changed and that the constraints have been adapted to a scenario tree representation of uncertainty. We indeed consider a stochastic framework similarly as in the previous model. Also, as the design decisions have been made in Chapter 3 the variables related these decisions have now been considered as parameters of the problem. The perfect foresight model that will be compared with this model is very similar to Model 7. The only difference is the fact that we optimize over a set of scenarios instead of the complete scenario tree. This model is convex and can, as stated previously, be solved with standard solvers. We have the guarantee that every local optimal solution will be a global optimal solution.

4.6 Results

Both the real time pricing model and the perfect foresight model have been tested using the test case from 4.3 and the same computer as in Chapter 3. Again, this has been implemented using programming language `AMPL` using the `Gurobi` solver with the default barrier algorithm. The computation times are given in Table 4.5.

Time	Real time	Perfect foresight
`_ampl_time`	17.55 s	20.03 s
`_solve_time`	154.52 s	235.29 s

Table 4.5: Computation times for solving Model 7 with the test case of Section 4.3.

4.6.1 Behavior: real time vs. perfect foresight

Let us first have a look at Figure 4.7. We see that the average storage profiles of both

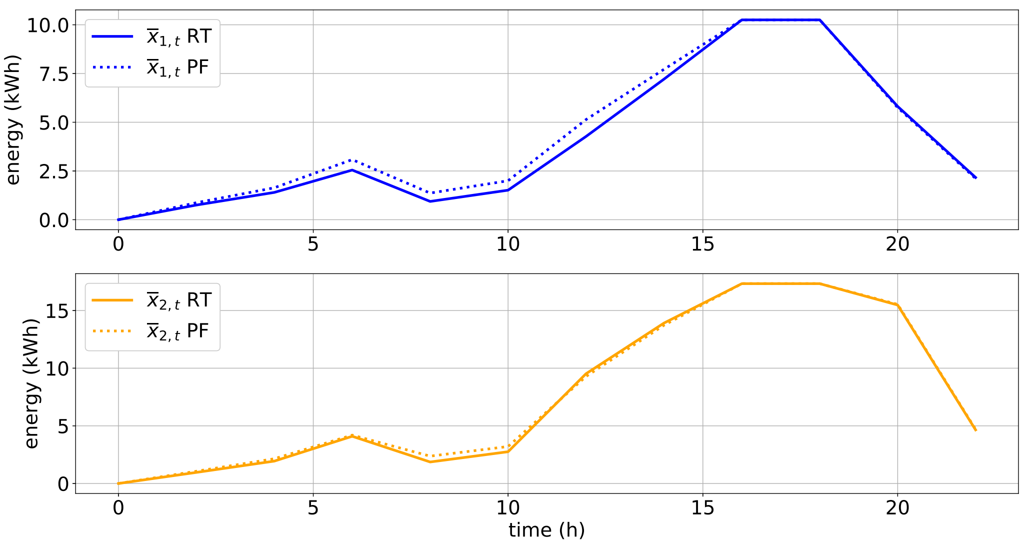

Figure 4.7: Average battery storage comparison between perfect foresight and real time pricing.

nodes for both batteries are very similar. They are also analogous to the the storage profiles presented in Figure 3.5. This was predictable as the daily production cost of Model 5 corresponds to the objective of the considered perfect foresight model. Again, two charging periods can be identified corresponding to an anticipation of higher demand in future time stages. A small difference in average battery level at the start of the horizon can however be observed depending on the model used. This is due to the fact that the perfect foresight model exactly knows what the future PV output power will be which is not the case for the real time pricing model.

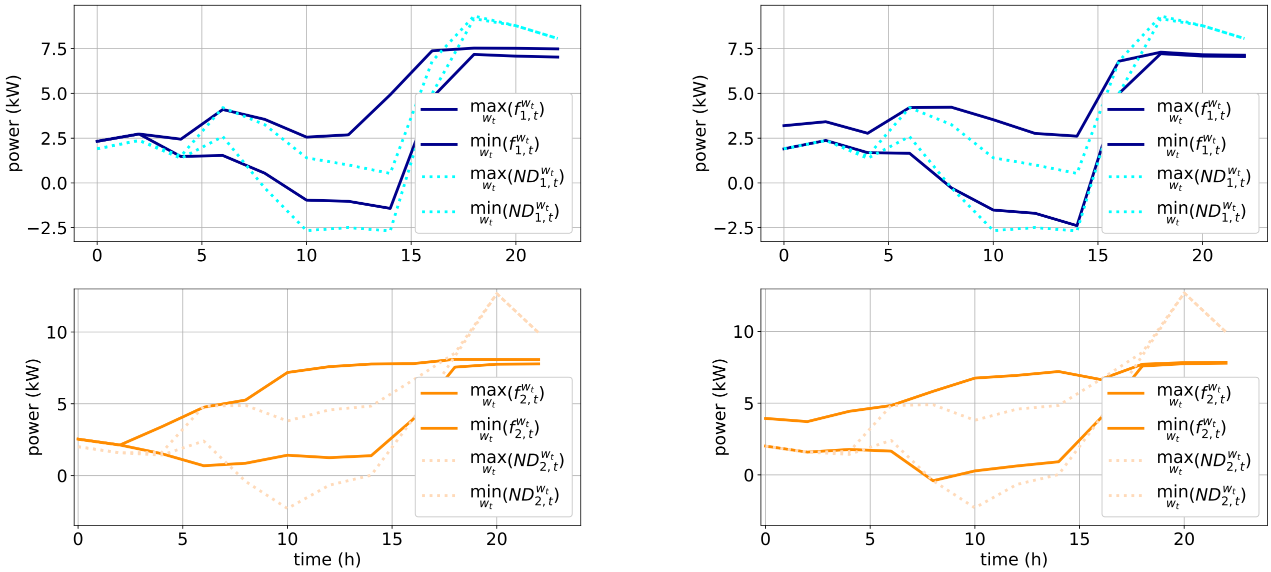

(a) Real time

(b) Perfect foresight

Figure 4.8: Comparison of the maximal and minimal flow going to the leaf node with maximal and minimal net demand.

This is illustrated in Figure 4.8 where it can easily be seen that bigger fluctuations in flow exist at the start of the horizon for the perfect foresight model compared to the real time pricing model. The maximal flow of the real time pricing model is therefore higher during subsequent time steps. Whereas the minimal flow of the perfect foresight model is lower during subsequent time steps due to planned exchange between leaf nodes in some sampled scenarios.

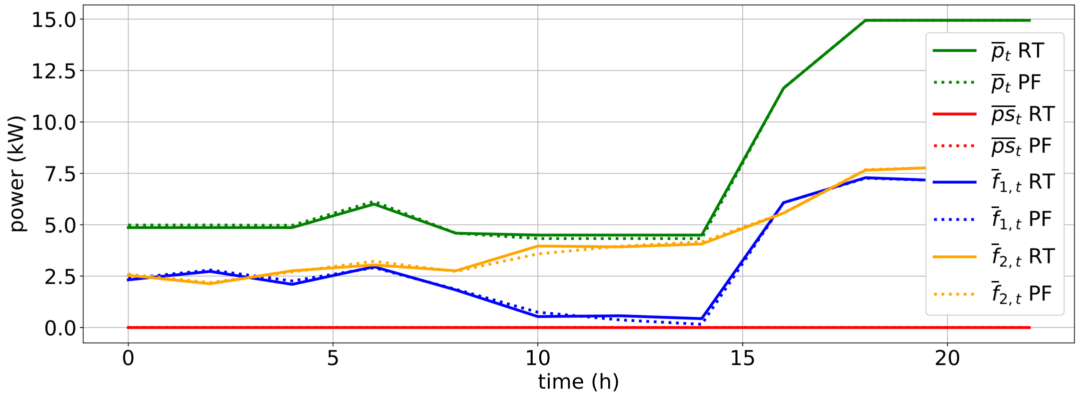

Figure 4.9: Average customer behavior and the influence on the root node when using real time pricing compared to perfect foresight.

The withdrawn power from the transmission lines can be observed in Figure 4.9. The battery is thus used to store excess PV supply and in order to cope with higher demand throughout the day. This will have the benefit of reducing peak loads and thus reduce costs because of the quadratic shape of the production cost function.

4.6.2 Price

We are able to get the average optimal interface price using the dual variables of the optimal solution of Model 7 as shown in Figure 4.10. We see that both models behave very similarly in terms of average interface price. It is first important to note that the interface price is the same for all nodes in both models thus explaining why only one graph is shown.

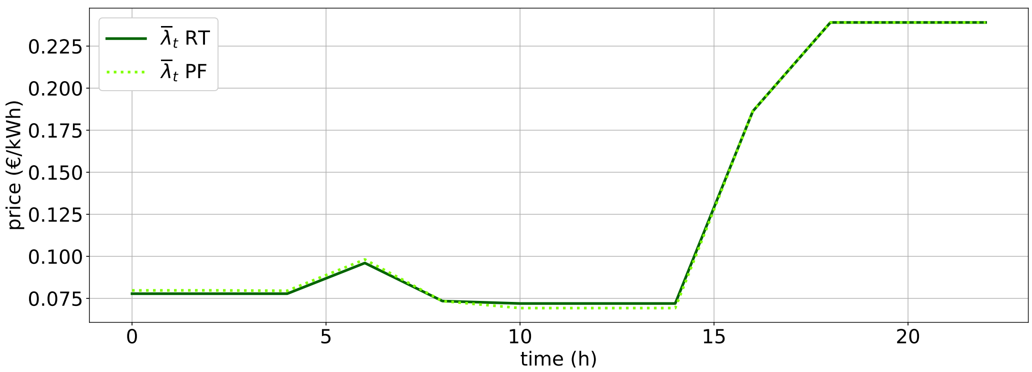

Figure 4.10: Average interface price for perfect foresight and real time pricing.

Four periods can be identified. At the start of the horizon we see that the price is low in order to allow both nodes to charge their batteries for the upcoming demand. Then, the battery is in average discharged at 6 am in both nodes explaining why a price spike can be observed.

The interface price then decreases to encourage both nodes to store energy in their batteries in order to anticipate higher demand. Finally, a high interface price is chosen to induce both nodes to use their batteries and sell excess PV power if available. The high price at the end of the horizon is also explained by the fact that the battery cannot be filled more before the evening as shown in Figure 4.7 thus implying that more power has to be produced during the last time stages. This results in a higher marginal cost of power production at the end of the horizon due to the quadratic nature of the production cost function.

4.6.3 Network

From a network point of view Table 4.6 shows that real time pricing behaves better compared to the previously considered pricing methods. This could be expected as the system has been designed specifically from a system point of view thus favoring the real time pricing results.Whether it is in terms of production cost, leaf node payment, average power shedding or congestion of the lines we see that this method works better than the other two methods.

Feature	Flat rate	Time of use	Real time	Perfect foresight
Leaf nodes				
Average payment of node 1	21.28 €	19.50 €	15.28 €	14.91 €
Average payment of node 2	27.79 €	25.94 €	17.92 €	17.40 €
Root node				
Average power shedding	8.48 kWh	8.49 kWh	0 kW	0 kW
Average power consumption	192.12 kWh	197.95 kWh	190.28 kWh	190.24 kWh
Average production cost	11.10 €	12.12 €	8.30 €	8.08 €
Lines				
Congestion % node 1	25.00 %	25.00 %	0 %	0 %
Congestion % node 2	25.00 %	25.01 %	0 %	0 %
F for 90 % prob. of uncongested line node 1	8.77 kW	8.77 kW	7.15 kW	7.15 kW
F for 90 % prob. of uncongested line node 2	9.94 kW	12.68 kW	7.82 kW	7.81 kW
F for 95 % prob. of uncongested line node 1	9.32 kW	9.23 kW	7.29 kW	7.26 kW
F for 95 % prob. of uncongested line node 2	12.68 kW	13.34 kW	7.86 kW	7.84 kW
F for 100 % prob. of uncongested line node 1	9.32 kW	9.33 kW	7.53 kW	7.30 kW
F for 100 % prob. of uncongested line node 2	12.68 kW	13.50 kW	8.10 kW	7.85 kW

Table 4.6: Network influence comparison between all pricing methods.

Next, we see that the network performance of real time is not far away from perfect foresight. A slight difference in leaf node payment and production cost can be observed, as explained before. This is because perfect foresight has exact knowledge about the upcoming PV power output allowing the model to smooth the power produced over the horizon, slightly decreasing the objective function. The system has also been over designed for perfect foresight as the line capacities are never reached. This is due to the fact that we went from a 15 minute interval to a 2 hour interval between time steps reducing the chance of having power spikes.

From an ecological point of view, we finally see that real time pricing never sheds power and needs less power to satisfy the demand compared to flat rate and time of use pricing.

Conclusion

An economical study of distribution systems is presented in this thesis.

At first, a typical distribution system is studied and a way of generating typical distribution system instances is proposed.

Then, a new framework for designing and analyzing distribution systems is presented. A multi-stage stochastic program is deduced from the considered framework and solved using typical distribution system data. Finally, the consequences of the customer's reaction are studied for three different retail pricing methods.

We have answered the following three questions that where addressed in the introduction.

1. **How should a low voltage sub network be optimally designed in order to maximize the power system welfare?**

   From a system welfare maximization point of view battery capacity should be prioritized to line capacity. As shown in Chapter 3 battery capacity can be used to reduce the need for expensive lines. However, reducing line capacity increases the risk of congesting the distribution lines. A trade off has thus to be made between both technologies. One also has to keep in mind that no battery capacity can be installed by the DSO of the system meaning that BESS's will have to be installed in households. This allows customers to control their interaction with the grid at their own will enabling them to minimize their monthly payment at the expense of system welfare maximization.

2. **How will distribution system customers equipped with a PV system and a BESS react to different retail pricing options?**

   The behavior of consumers is studied for three retail pricing options. It will be very similar when flat rate and time of use pricing are applied. It can be concluded that in both cases the low voltage clusters will send all excess PV power to the root node. One difference remains in the fact that for time of use pricing consumers will fully charge their battery in order for them to discharge it during the day. This is not the case for flat rate pricing where the battery will never be used by the customers. These deductions show that for these two pricing methods the battery will never be used to store excess PV power contradicting the initial purpose of installing a battery. For real time pricing however a general trend can be observed with respect to BESS management; The battery of each leaf node is filled using excess PV output and complementary power coming from transmission lines as a provision for high demand periods in order to smooth the power demand coming from transmission lines and avoid congestion.

3. **What are the consequences from a network point of view of high RES penetration at consumer level?**

   If high PV power penetration on the grid is considered we have shown that excessive power shedding might represent a dangerous consequence if traditional retail tariff methods are still applied. Indeed as LV sub networks connected to the same feeder are always situated in the same area this will induce that on sunny days all LV networks will simultaneously send all their excess PV power resulting in high power shedding. This issue can however be bypassed by using real time pricing. Real time pricing has often been referred to the future of retail pricing in distribution systems but is still very difficult to implement in practice. We have seen that real time pricing behaves better both from an system welfare and ecological point of views.

Future directions

Many improvements can be made in order to enhance the results of this Master thesis. First of all, as stated before we have made the assumption that leaf nodes represent aggregates of consumers. In reality this is not the case and implies that in Chapter 3 approximations have to be made regarding the line capacity investment cost connecting the leaf nodes with the root node. A more developed model could have been made by removing the leaf node aggregate assumption which would allow us to study more in depth the interactions between individual consumers. Having made linear assumptions about the power flow constraints this would also allow more detailed power flow equations to be considered. However, the computation time would highly suffer from these improvements.

Next, the assumption has been made that the PV panels of both leaf nodes output the same amount of power. However, this is not the case in reality. The output of these PV panels should indeed be highly correlated but not equal to each other. This could be coupled with the addition of considering more leaf nodes connected to the root node. Adding these features to the model would give us more realistic results but would highly increase solve times as this increases the size of the considered scenario tree. Indeed, one node of the scenario tree would have to be created for each possible combination of PV output of all leaf nodes.

A totally different approach based on bilevel programming would also be an alternative to consider. The leader would then be the retailer deciding the optimal retail prices and design of the LV sub networks. The customer would therefore be the follower trying to minimize his payment. This could then be combined with a demand response model describing the customer behavior in a more detailed way.

Finally, in Chapter 4 more time steps should be considered in order to get a more detailed description of the behavior of customers. We have used 12 time steps which means a decision is made every 2 hours which is not representative of reality. Increasing this parameter would however force us to use methods such as Stochastic Dual Programming [26] and Model Predictive Control [27] which have already proven their effectiveness on many similar applications.

Appendices

Appendix A

Generation of realistic distribution system instances

A.1 Voltage level clustering algorithm

Algorithm 1: Voltage Level Clustering.

Input : T : set of buses connected to at least one transformer, B : set of all buses,
$n : B \to A \subseteq B$: function that returns all the neighbors of the input bus,
$i : T \to \mathbb{R}_+$: function that returns the voltage of the transformer bus.
Output: C : set of clusters that contain buses of a certain voltage level, v_i : voltage of cluster c_i.

```
while T ≠ ∅ do
    Choose t in T;
    T ← T \ {t};
    N_1 ← n(t);
    c_i ← {t};
    v_i ← i(t);
    while N_1 ≠ ∅ do
        N_2 ← ∅;
        for p ∈ N_1 do
            c_i = c_i ∪ {p};
            if n ∈ T then
                T ← T \ {p};
            end
            N_2 ← N_2 ∪ (n(p) \ (N_1 ∪ c_i));
        end
        N_1 ← N_2;
    end
    C ← C ∪ {c_i};
end
```

A.2 Prim's minimum spanning tree algorithm

Algorithm 2 gives us the minimum spanning tree of graph (V, E) in $\mathcal{O}(|V|^2)$ time [19]. The maximum spanning tree can also easily be obtained using the same algorithm. It suffices to apply the algorithm on the same graph with negated weights.

Algorithm 2: Prim's minimum spanning tree algorithm.

Input : V : set of vertices, E : set of edges, $w : E \to \mathbb{R}$: weight associated to each edge $(v_i, v_j) \in E$.
Output: Minimum weight spanning tree of (V, E).

```
U ← {v_1};
T ← ∅;
for v ∈ V \ {v_1} do
    closest_v ← v_1;
end
while U ≠ V do
    for v ∈ V \ U do
        if w(v, closest_v) < min then
            min ← w(v, closest_v);
            next ← v;
        end
    end
    U ← U ∪ {next};
    T ← T ∪ {(next, closest_next)};
    for v ∈ V \ U do
        if w(v, closest_v) > w(v, next) then
            closest_v ← next;
        end
    end
end
```

A.3 Low voltage templates

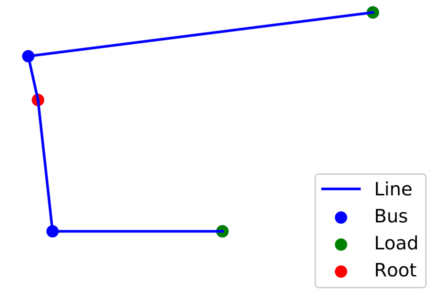

(a) 5 node template LV cluster

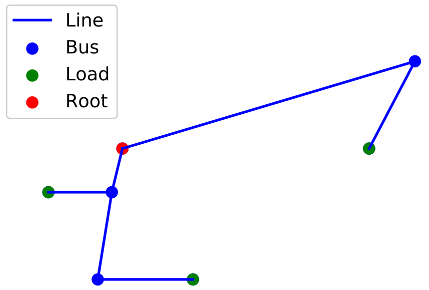

(b) 7 node template LV cluster

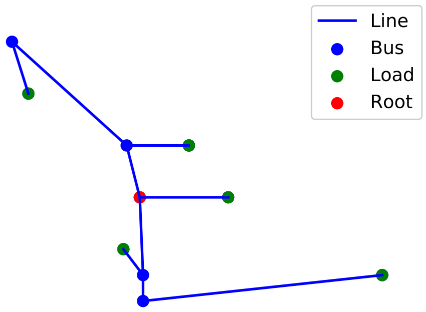

(c) 10 node template LV cluster

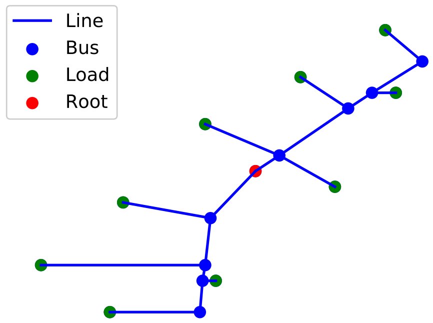

(d) 18 node template LV cluster

Figure A.1: Low voltage clusters.

Appendix B

Design of distribution systems: a new framework

B.1 Optimization model nomenclature

Data

- $T = \{0, \dots, H\}$: Set of considered time stages.
- Δt : Interval between two time steps.
- $\Omega_{[t]}$: Set of scenarios at time stage t.
- $S \subseteq \Omega_{[H]}$: Subset of scenarios sampled randomly.
- $L = \{1, 2\}$: Set of leaf nodes.
- $\mathrm{D}_{l,t}$: Demand of node n at time step t.
- RP_t^s : Renewable power production of one PV system in sampled scenario s of time step t.
- Sys_l : Number of PV systems in leaf node l.
- $I = \{\text{line capacity, battery energy capacity, battery charge/discharge rate}\}$: Set of infrastructures.
- $\mathrm{TC}(p_t^s) : \mathbb{R}_+ \rightarrow \mathbb{R}_+$: Hourly total production cost.
- VOLL Hourly value of lost loads.
- IC_i Investment cost of the creation of a distribution network of a certain capacity in node n.
- LT_i: Lifetime of component i.

- μ : Battery discharging efficiency.
- η : Battery charging efficiency.
- κ : C-rate of the battery.
- r : Discount rate.

Variables

- $x_{l,t}^{s} \in \mathbb{R}$: Energy stored in node l in sampled scenario s at time step t.
- $f_{l,t}^{s} \in \mathbb{R}$: Power sent/received by node 3 to/from node l in sampled scenario s at time step t.
- $bc_{l,t}^{s} \in \mathbb{R}$: Power added in the battery of node l in sampled scenario s at time step t.
- $bd_{l,t}^{s} \in \mathbb{R}$: Power extracted from the battery in node l in sampled scenario s at time step t.
- $p_{t}^{s} \in \mathbb{R}$: Power withdrawn from transmission lines in sampled scenario s at time step t.
- $ps_{l,t}^{s} \in \mathbb{R}$: Excess power shed in sampled scenario s at time step t at node l.
- $ls_{l,t}^{s} \in \mathbb{R}$: Excess load shed in sampled scenario s at time step t at node l.
- R_l : Maximal charge/discharge rate of the battery in leaf node l.
- C_l : Maximal capacity of the battery in leaf node l.
- F_l : Maximal power sent/received to/from leaf node l.

Appendix C

Influence of retail pricing on customers and network congestion

C.1 Test case

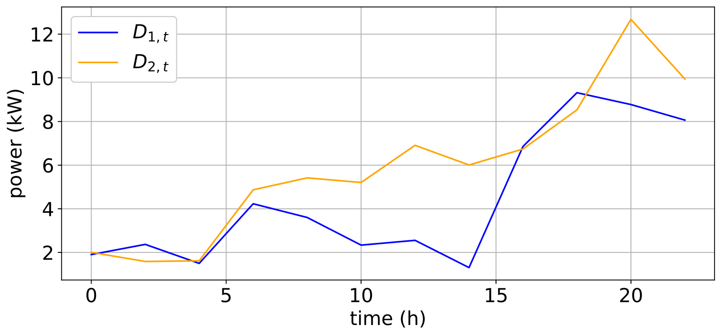

Figure C.1: Demand profiles of the leaf nodes in the experimental setup.

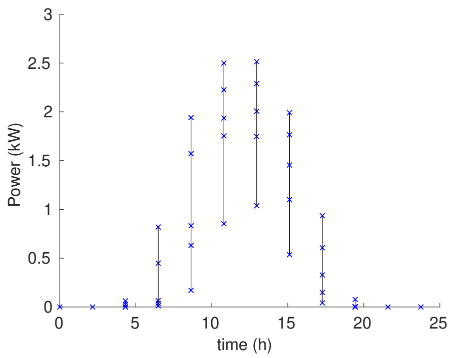

Figure C.2: Lattice nodes generated for the lattice model.

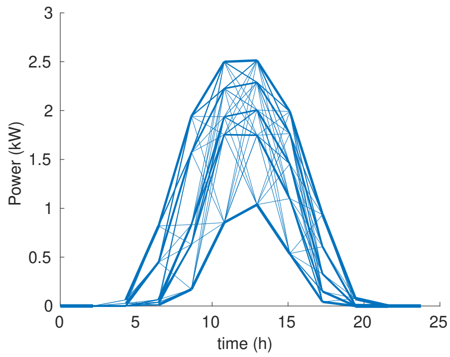

Figure C.3: Set of 5000 samples generated by the scenario generator using the lattice model.

Bibliography

[1] Anthony Papavasiliou. Lecture notes in quantitative energy economics, January 2019.

[2] Erkki Lakervi and Edward J Holmes. *Electricity distribution network design*. Number 21. IET, 1995.

[3] Anthony Papavasiliou. Lecture notes in operational research, January 2019.

[4] Conditions et fiches de prix. `https://www.electrabel.be/fr/particulier/prices-and-conditions`. Accessed: 2015-12-28.

[5] AG Energiebilanzen. Bruttostromerzeugung in deutschland ab 1990 nach energieträgern. *Stand*, 11:2015, 2015.

[6] Tien Ming Lee, Ezra M Markowitz, Peter D Howe, Chia-Ying Ko, and Anthony A Leiserowitz. Predictors of public climate change awareness and risk perception around the world. *Nature climate change*, 5(11):1014, 2015.

[7] Fouad Abou Chacra, Patrick Bastard, Gilles Fleury, and Régine Clavreul. Impact of energy storage costs on economical performance in a distribution substation. *IEEE Transactions on Power Systems*, 20(2):684–691, 2005.

[8] I. Ziari, G. Ledwich, A. Ghosh, and G. Platt. Optimal distribution network reinforcement considering load growth, line loss, and reliability. *IEEE Transactions on Power Systems*, 28(2):587–597, May 2013.

[9] Eloy Díaz-Dorado, José Cidrás Pidre, and Edelmiro Míguez García. Planning of large rural low-voltage networks using evolution strategies. *IEEE Transactions on Power Systems*, 18(4):1594–1600, 2003.

[10] L Moretti, S Polimeni, L Meraldi, P Raboni, S Leva, and G Manzolini. Assessing the impact of a two-layer predictive dispatch algorithm on design and operation of off-grid hybrid microgrids. *Renewable Energy*, 2019.

[11] A. Navarro-Espinosa and L. F. Ochoa. Probabilistic impact assessment of low carbon technologies in lv distribution systems. *IEEE Transactions on Power Systems*, 31(3):2192–2203, May 2016.

[12] S Borenstein, M Jaske, and A Ros. Dynamic pricing, advanced metering, and demand response in electricity markets. *Journal of the American Chemical Society*, 128:4136–4145, 01 2002.

[13] Paul L Joskow and Catherine D Wolfram. Dynamic pricing of electricity. *American Economic Review*, 102(3):381–85, 2012.

[14] M. Asensio, G. Muñoz-Delgado, and J. Contreras. Bi-level approach to distribution network and renewable energy expansion planning considering demand response. *IEEE Transactions on Power Systems*, 32(6):4298–4309, Nov 2017.

[15] Doug F Warne. *Newnes electrical power engineer's handbook*. Elsevier, 2005.

[16] Per J Agrell and Jonas Teusch. Making the belgian distribution system fit for the energy transition. *Reflets et perspectives de la vie économique*, 54(1):157–174, 2015.

[17] Bay area synthetic network. `https://egriddata.org/dataset/bay-area-synthetic-network`. Accessed: 04-05-2019.

[18] Venkat K Krishnan, Bryan S Palmintier, Brian S Hodge, Elaine T Hale, Tarek Elgindy, Bruce Bugbee, Michael N Rossol, Anthony J Lopez, Dheepak Krishnamurthy, Claudio Vergara, Carlos Mateo Domingo, Fernando Postigo, Fernando de Cuadra, Tomas Gomez, Pablo Duenas, Max Luke, Vivian Li, Mohan Vinoth, and Sree Kadankodu. Smart-ds: Synthetic models for advanced, realistic testing: Distribution systems and scenarios.

[19] C.H. Papadimitriou and K. Steiglitz. *Combinatorial Optimization: Algorithms and Complexity*. Dover Books on Computer Science. Dover Publications, 1998.

[20] Alejandro Navarro-Espinosa and Luis F Ochoa. Probabilistic impact assessment of low carbon technologies in lv distribution systems. *IEEE Transactions on Power Systems*, 31(3):2192–2203, 2015.

[21] A. Papavasiliou, S. S. Oren, and R. P. O'Neill. Reserve requirements for wind power integration: A scenario-based stochastic programming framework. *IEEE Transactions on Power Systems*, 26(4):2197–2206, Nov 2011.

[22] Yurii Nesterov. *Introductory lectures on convex optimization: A basic course*, volume 87. Springer Science & Business Media, 2013.

[23] Ian Richardson, Murray Thomson, David Infield, and Conor Clifford. Domestic electricity use: A high-resolution energy demand model. *Energy and buildings*, 42(10):1878–1887, 2010.

[24] Zhouyang Ren, Wei Yan, Xia Zhao, Wenyuan Li, and Juan Yu. Chronological probability model of photovoltaic generation. *IEEE Transactions on Power Systems*, 29(3):1077–1088, 2013.

[25] Cdistributed generation interconnection program data. https://www.californiadgstats.ca.gov/downloads/#_csi_15_id. Accessed: 2019-05-10.

[26] Mario VF Pereira and Leontina MVG Pinto. Multi-stage stochastic optimization applied to energy planning. *Mathematical programming*, 52(1-3):359–375, 1991.

[27] Jacob Mattingley, Yang Wang, and Stephen Boyd. Receding horizon control. *IEEE Control Systems*, 31(3):52–65, 2011.

UNIVERSITÉ CATHOLIQUE DE LOUVAIN
École polytechnique de Louvain
Rue Archimède, 1 bte L6.11.01, 1348 Louvain-la-Neuve, Belgique | **www.uclouvain.be/epl**